OPEN ACCESS

# African Journal of Environmental Science and Technology

December 2023
ISSN 1996-0786
DOI: 10.5897/AJEST
www.academicjournals.org

ACADEMIC JOURNALS
expand your knowledge

## About AJEST

African Journal of Environmental Science and Technology (AJEST) provides rapid publication (monthly) of articles in all areas of the subject such as Biocidal activity of selected plant powders, evaluation of biomass gasifier, green energy, Food technology etc. The Journal welcomes the submission of manuscripts that meet the general criteria of significance and scientific excellence. Papers will be published shortly after acceptance. All articles are peer-reviewed

**Indexing**

The African Journal of Environmental Science and Technology is indexed in:
CAB Abstracts, CABI's Global Health Database, Chemical Abstracts (CAS Source Index), China National Knowledge Infrastructure (CNKI), Dimensions Database, Google Scholar, Matrix of Information for The Analysis of Journals (MIAR), Microsoft Academic

AJEST has an h5-index of 14 on Google Scholar Metrics

**Open Access Policy**

Open Access is a publication model that enables the dissemination of research articles to the global community without restriction through the internet. All articles published under open access can be accessed by anyone with internet connection.

The African Journal of Environmental Science and Technology is an Open Access journal. Abstracts and full texts of all articles published in this journal are freely accessible to everyone immediately after publication without any form of restriction.

**Article License**

All articles published by African Journal of Environmental Science and Technology are licensed under the Creative Commons Attribution 4.0 International License. This permits anyone to copy, redistribute, remix, transmit and adapt the work provided the original work and source is appropriately cited. Citation should include the article DOI. The article license is displayed on the abstract page the following statement:

This article is published under the terms of the Creative Commons Attribution License 4.0
Please refer to https://creativecommons.org/licenses/by/4.0/legalcode for details about Creative Commons Attribution License 4.0

**Article Copyright**

When an article is published by in the African Journal of Environmental Science and Technology, the author(s) of the article retain the copyright of article. Author(s) may republish the article as part of a book or other materials. When reusing a published article, author(s) should; Cite the original source of the publication when reusing the article. i.e. cite that the article was originally published in the African Journal of Environmental Science and Technology. Include the article DOI Accept that the article remains published by the African Journal of Environmental Science and Technology (except in occasion of a retraction of the article) The article is licensed under the Creative Commons Attribution 4.0 International License.

A copyright statement is stated in the abstract page of each article. The following statement is an example of a copyright statement on an abstract page.
Copyright ©2016 Author(s) retains the copyright of this article.

**Self-Archiving Policy**

The African Journal of Environmental Science and Technology is a RoMEO green journal. This permits authors to archive any version of their article they find most suitable, including the published version on their institutional repository and any other suitable website.
Please see http://www.sherpa.ac.uk/romeo/search.php?issn=1684-5315

**Digital Archiving Policy**

The African Journal of Environmental Science and Technology is committed to the long-term preservation of its content. All articles published by the journal are preserved by Portico. In addition, the journal encourages authors to archive the published version of their articles on their institutional repositories and as well as other appropriate websites.
https://www.portico.org/publishers/ajournals/

**Metadata Harvesting**

The African Journal of Environmental Science and Technology encourages metadata harvesting of all its content. The journal fully supports and implement the OAI version 2.0, which comes in a standard XML format. See Harvesting Parameter

# Memberships and Standards

Academic Journals strongly supports the Open Access initiative. Abstracts and full texts of all articles published by Academic Journals are freely accessible to everyone immediately after publication.

All articles published by Academic Journals are licensed under the Creative Commons Attribution 4.0 International License (CC BY 4.0). This permits anyone to copy, redistribute, remix, transmit and adapt the work provided the original work and source is appropriately cited.

Crossref is an association of scholarly publishers that developed Digital Object Identification (DOI) system for the unique identification published materials. Academic Journals is a member of Crossref and uses the DOI system. All articles published by Academic Journals are issued DOI.

Similarity Check powered by iThenticate is an initiative started by CrossRef to help its members actively engage in efforts to prevent scholarly and professional plagiarism. Academic Journals is a member of Similarity Check.

CrossRef Cited-by Linking (formerly Forward Linking) is a service that allows you to discover how your publications are being cited and to incorporate that information into your online publication platform. Academic Journals is a member of CrossRef Cited-by.

Academic Journals is a member of the International Digital Publishing Forum (IDPF). The IDPF is the global trade and standards organization dedicated to the development and promotion of electronic publishing and content consumption.

## Contact

Editorial Office: ajest@academicjournals.org

Help Desk: helpdesk@academicjournals.org

Website: http://www.academicjournals.org/journal/AJEST

Submit manuscript online http://ms.academicjournals.org

Academic Journals
73023 Victoria Island, Lagos, Nigeria
ICEA Building, 17th Floor,
Kenyatta Avenue, Nairobi, Kenya.

## Editors

**Dr. Guoxiang Liu**
Energy & Environmental Research Center (EERC)
University of North Dakota (UND)
North Dakota 58202-9018
USA

**Prof. Okan Külköylüoglu**
Faculty of Arts and Science
Department of Biology
Abant Izzet Baysal University
Turkey.

**Dr. Abel Ramoelo**
Conservation services,
South African National Parks,
South Africa.

## Editorial Board Members

**Dr. Manoj Kumar Yadav**
Department of Horticulture and Food Processing
Ministry of Horticulture and Farm Forestry
India.

**Dr. Baybars Ali Fil**
Environmental Engineering
Balikesir University
Turkey.

**Dr. Antonio Gagliano**

Department of Electrical, Electronics and Computer Engineering
University of Catania
Italy.

**Dr. Yogesh B. Patil**
Symbiosis Centre for Research & Innovation
Symbiosis International University
Pune,
India.

**Prof. Andrew S Hursthouse**
University of the West of Scotland
United Kingdom.

**Dr. Hai-Linh Tran**
National Marine Bioenergy R&D Consortium
Department of Biological Engineering
College of Engineering
Inha University
Korea.

**Dr. Prasun Kumar**
Chungbuk National University,
South Korea.

**Dr. Daniela Giannetto**
Department of Biology
Faculty of Sciences
Mugla Sitki Koçman University
Turkey.

**Dr. Reem Farag**
Application department,
Egyptian Petroleum Research Institute,
Egypt.

# Table of Content

Vol. 17(12), pp. 302-312, December 2023
DOI: 10.5897/AJEST2023.3237
Article Number: 95DCC4B71569
ISSN: 1996-0786
Copyright ©2023
Author(s) retain the copyright of this article
http://www.academicjournals.org/AJEST

ACADEMIC JOURNALS
expand your knowledge

**African Journal of Environmental Science and Technology**

*Full Length Research Paper*

# Groundwater quality assessment and human health risks in Ovitoto, Otjozondjupa Region, Namibia

**Priskila Mwatukange[1], Erold Naomab[2] and Omotayo Rafiu Awofolu[1]***

[1]Department of Preventative Health Sciences, School of Health Sciences, Namibia University of Science and Technology, Windhoek, Namibia.
[2]Office of the Vice-Chancellor, Namibia University of Science and Technology, Windhoek, Namibia.

Received 9 October, 2023; Accepted 23 November, 2023

**Namibia, a dry country relies heavily on groundwater resources which is susceptible to anthropogenic contamination. The study assessed the quality and health risks of borehole water supplied to residents of the Ovitoto community in Otjozondjupa region of Namibia. Water samples were collected from nine boreholes across nine communities over a period of six months and subjected to physicochemical and microbial analyses. Heavy metals were extracted using mineral acid digestion and detected using Inductively Coupled Plasma Optical Emission spectroscopy (ICP-OES). Microbial entities were analyzed using standard bacteriological method. Results revealed that the pH, temperature, and electrical conductivity (EC) of samples were within WHO permissible levels for human consumption while Turbidity and total dissolved solids (TDS) were above the limit. Overall mean concentrations of heavy metals were 0.83, 0.01, 0.02, 17.8, and 7.09 mg/L for Zn, Cd, Pb, Fe, and Mn respectively. WHO drinking water permissible levels were obtained for Cd, Pb, Fe and Mn and the water could also be regarded as unsuitable for irrigational use because it is above permissible levels of Cd, Fe, and Mn. Zn and Cd showed a strong correlation (r=0.99) with an average correlation (r=0.55) between Cd and Cu. The human health risk of the metals was assessed using the Target Hazard Quotient (THQ) and Carcinogenic Risk Index (CRI), where HQ >1 and CRI > 1.0×10-4 indicate non-carcinogenic and carcinogenic risks, respectively. THQ values < 1 was obtained for analyzed metals in both children and adults. However, CRI (Mn) values of 4.8 for adults and 18.1 for children indicate potential exposure to carcinogenic risk. Detection of HPC, Tc, and Fc in water samples above permissible levels also gives cause for concern. Pretreatment and monitoring of borehole water samples before distribution for consumption is highly recommended.**

**Key words:** Water quality, human health, health risks, groundwater, Namibia.

## INTRODUCTION

Clean and safe drinking water is regarded as an essential resource for human survival and has been recognized, globally as a fundamental human right (UNGA, 2015, 2016). Yet, about 1 in 3 people globally do not have access to safe drinking water (WHO, 2019). Given the diminishing availability of this critical resource due to compounding

*Corresponding author. E-mail: oawofolu@nust.na. Tel: +264612072500.

Author(s) agree that this article remain permanently open access under the terms of the Creative Commons Attribution License 4.0 International License

natural (geological, geomorphological formation, and bedrock-water-interaction) and anthropogenic (agricultural, industrial, and climatic) factors (Nagaraju et al., 2016), several countries have resorted to alternative processes such as groundwater abstraction (Foteinis and Masindi, 2021) and seawater desalination (Dhakal et al., 2022). In many rural communities of the developing countries, the main source of water for drinking and other domestic activities is the groundwater.

Due to a lack of access to modern machinery for the installation of boreholes with an average geological depth of between 100 and 150 m that can supply relatively cleaner and more potable water, rural community members usually use manual and less effective tools in creating and accessing groundwater commonly referred to as “wells” with depth varying between 6 and 9 m depending on groundwater level. Notwithstanding the depth of the groundwater source, the quality of water therefrom can become degraded as a result of pollution from point and non-point sources (UNEP, 2010; Daly et al., 2021; Ye et al., 2022).

Aquifers can become vulnerable to pollution due to disturbances and changes to the physical topography resulting from human activities such as road construction and mining which may further alter the hydrological dynamics of the groundwater (Mulyadi et al., 2020). Furthermore, the disposal of domestic and agricultural solid wastes containing contaminants such as detergents, heavy metals, and other organic pollutants on land can result in the leaching of these toxic chemicals into the soil with potential contamination of the groundwater. The deterioration of groundwater quality has been linked to landfill leachate with elevated Pollution Load Index (PLI = 29.14), which was above the permissible limits for the discharge of leachate (Fadili et al., 2022a). In a related study, the quality of groundwater was found to have been compromised by heavy metals-enriched soil in the vicinity of municipal solid waste dumpsites with moderate to high contamination levels (PLI = 1.84) (Fadili et al., 2022b). The application of the Water Quality Index (WQI) for assessing the quality of groundwater resources revealed that about 98.9% of analyzed water samples were contaminated (Khaneghah et al., 2020).

Due to cost, many subsistent farmers in the study area are known to use relatively cheap and toxic pesticides that are not environmentally friendly with serious long-term human health effects. Modern, biodegradable pesticides are usually more expensive and unaffordable for many of the rural farmers. The presence of toxic pesticides and other contaminants in groundwater sources has been reported (Bexfield et al., 2021). Generally, communal/ subsistence and commercial agricultural practices are common in many communities in the country as a source of livelihood.

The dry and arid climatic condition of Namibia makes it susceptible to water scarcity and drought across all regions of the country including the Otjozondjupa region in which the study area is located. Hence, many communities utilize groundwater from boreholes as a freshwater source to address the issue of water scarcity for agricultural and domestic use. However, there are growing concerns about groundwater quality in most municipal areas. This stemmed from the observation of incessant blockage of the water pipe network by particulate matter at residences in the community. Hence, the rationale for the borehole water quality assessment across the community. The governmental agency, Namibia Water Corporation was also interested in the assessment since the oversight of water quality management is within the mandate of the agency. Apart from the impact of anthropological factors on groundwater quality, the contribution from the prevailing geological formation of the area, the rate of recharge, and the reflux of water have been reported (Ahamad et al., 2018).

The presence of background level of some inorganic substances such as iron, manganese, calcium, and zinc in groundwater sources as may be influenced by the geological formation is not uncommon. However, this level may become enriched due to anthropogenic activities that occur as a result of the deposition of solid and liquid wastes on soil. These wastes may potentially contain toxic substances such as heavy metals (Cd, Pb, As, Hg, and Cr), pathogenic entities (*Escherichia coli*), and pesticides. Agricultural, construction, and local industrial activities are prevalent in the study area, hence potential contamination of the groundwater is highly probable. The presence of these toxic substances in groundwater sources that did not undergo a rigorous water treatment process before consumption gives serious cause for concern. These toxic substances may find their way into the aquifer through percolation and leaching processes (Li et al., 2021).

Some studies have reported the contamination of groundwater as a result of the prevalence of pesticides (Herrero-Hernández et al., 2013), inorganic and organic substances (Singh et al., 2014), and microbial entities (Ifeanyi and Nwandkor, 2015). The preliminary physical observation of water samples from boreholes in conjunction with agricultural activities in the study area necessitates further examination of water from the boreholes in terms of their suitability for domestic use, in particular for drinking purposes. Hence, the aim of the study was an assessment of the quality and possible human health risks of borehole water at the Ovitoto community in the Otjozondjupa region, Namibia.

## MATERIALS AND METHODS

### Study area

Otjozondjupa region is located in the central part of Namibia. It has a total population of about 143,000 residents, with its capital at Otjiwarongo (NSA, 2013). The region is notable for cattle farming, livestock, and crop farming and is largely semi-arid with rainfall ranging from 300 to 600 mm, increasing from the southwest to the northeast. The climate condition of the area varies from arid to semi-

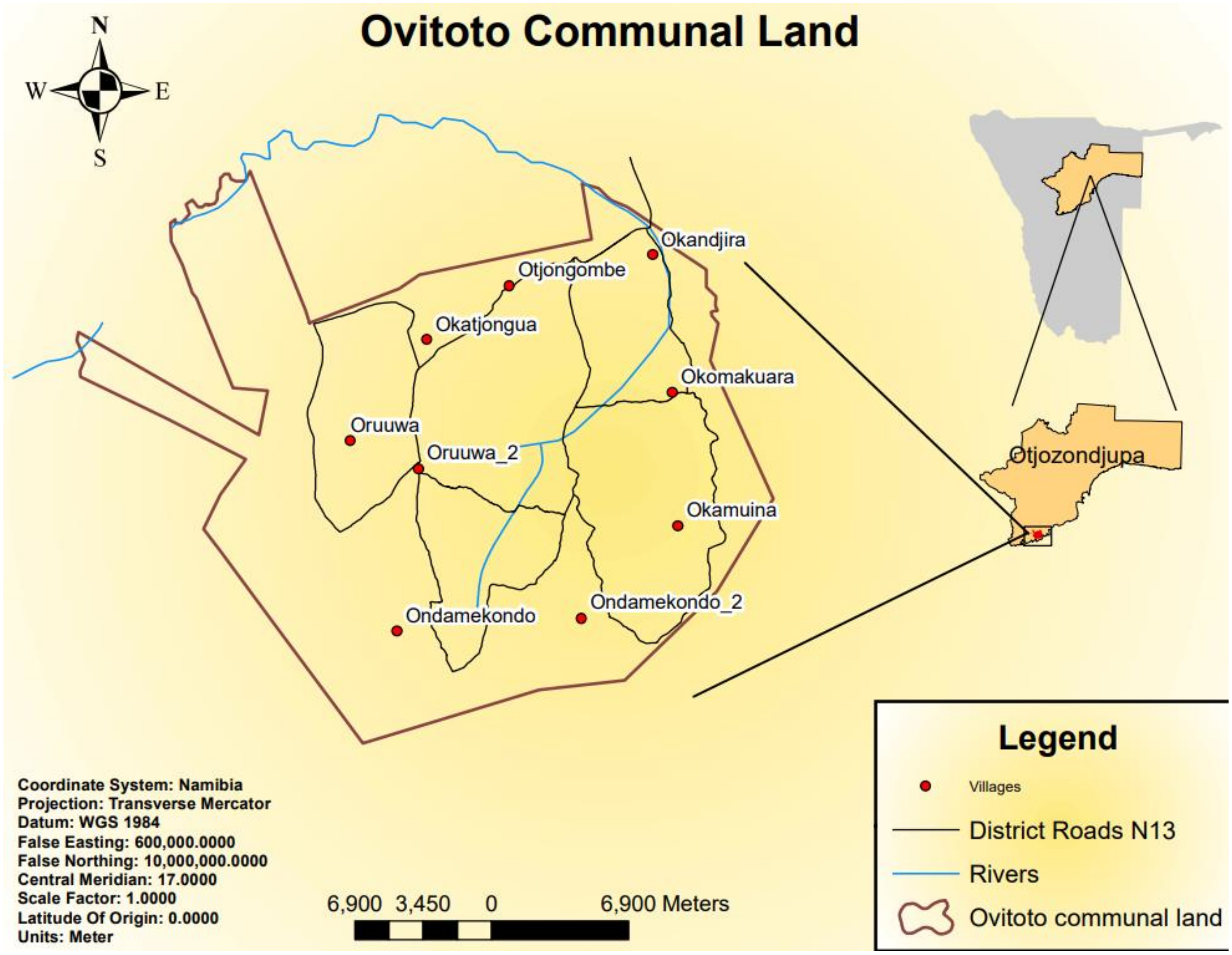


**Figure 1.** Map of Namibia and Otjozondjupa region (in set) and Ovitoto communal area showing sample collection points.

arid with an average day-day temperature of 33°C. Hence, the area is prone to annual droughts, making it peripheral for rain-fed crop production. The latitude and longitude of the area stand at -20.54869160, and the longitude is 17.66888700 (Latlong.Info, 2023).

Surface water resources are scarce and most of the communities depend on groundwater resources. Ovitoto municipal area within this region consists of nine communities namely Okasongua, Okomakuara, Okandjira, Ondamekondo, Okamuina, Ondamekondo 2, Oruuwa 01, Oruuwa 02, and Otjongombe. The average distance between each of the communities is about 6 km. The communities rely only on water supply from the boreholes which they use for all domestic activities including drinking. It is important to note that the water is utilized without any pretreatment. The map of the study area and sample collection points is presented in Figure 1.

### Sample collection, preparation, and storage

Groundwater samples were collected from nine selected boreholes as outlined by Alley (2000). Briefly, 1-L Nalgene plastic bottles were washed and stored in 10% nitric acid for 2 days and rinsed with double distilled water before usage for water sampling. The purpose of this cleaning regime was to ensure that the sampling containers were free from extraneous contaminants that may compromise the outcome of the analysis. Water samples were collected from the boreholes by first allowing the water to run for about 30 s, rinsing the bottle twice with a small portion of the water, and then filled to nearly full to allow for space. Sampling was carried out at almost the same time intervals across the sampling sites between the months of March and August 2022. Two water samples were collected per site on a monthly basis for six periods. Hence, a total of 108 water samples were collected across the sampling stations (Figure 2). All samples were appropriately labeled, kept cool at 4°C in a cooler box, and transported to the laboratory for further analysis. Samples were stored in the refrigerator at 4°C and analyzed within a 6 h period. Sampling bottles were marked on-site, where point names, locations, dates, times, and types of analysis to be conducted were recorded.

### Analytical methods

Physico-chemical parameters of water samples were determined on-site using a calibrated portable multi-parameter water quality meter with a serial number (HACH HI9828). These parameters are important in the assessment of drinking water quality as they provide a vital indication of suitability concerning human health and acceptability in terms of aesthetics and palatability.

Standard microbiological analytical methods were applied in the determination of the bacterial load of the water samples. The bacteriological assay involves analysis of Total coliform (*Tc*),

**Figure 2.** Pictures of some borehole water sampling sites.

Heterotrophic plate (HTC), and *E. coli*. Coliform bacteria have generally been utilized as standard microbiological indicators of the quality of drinking water due to the simplicity of the determination process (Osmani et al., 2019). They are rod-like in shape, Gram-negative bacteria that ferment lactose, producing acid and gas at 35 to 37°C within 24 to 48 h. They have been recognized as appropriate organisms and have long been recognized as a suitable microbial indicator of drinking water quality, largely because they are easy to detect and enumerate in water (Halkman, 2014).

Since the coliform count is inadequate for differentiation between fecal and non-fecal contamination; hence, fecal coliform (*E. coli*) analysis was carried out. *E. coli* is a member of the family Enterobacteriaceae and is characterized by the possession of the enzymes β-galactosidase and β-glucuronidase and grows at 44 to 45°C. They ferment the lactose in appropriate media (using Tryptone Bile Agar (TBX) in this study) with the production of acid and gas (Shaikhan et al., 2019). The WHO regulation, however, specifies zero limits for these indicators.

The heavy metal content in water samples was extracted using mineral acid digestion. Briefly, 100 ml of filtered (Whatman 0.45 µm filter paper) water samples were digested slowly on a hotplate using a mixture of 5 ml of concentrated nitric acid ($HNO_3$) and 5 ml of concentrated sulphuric acid ($H_2SO_4$) until the volume was reduced to about 20 ml. This was allowed to cool to room temperature, transferred to a 100 ml standard flask, and made up to mark with double distilled water. The metallic content of the digested water sample was analyzed using Inductively Couple-Plasma Optical Emission Spectroscopy (PerkinElmer, Optima 3000 ICP-OES System) following a previously described method (Cobbina et al., 2015). Quality assurance of the extraction process was through blank digest using the standard metal addition technique.

## Quantitative health risk assessment

Possible health risks that may be associated with the consumption of water samples were determined through the assessment of the following parameters.

### *Estimated daily intake (EDI)*

EDI = Metal conc. in water (mg/L) × Average daily water intake (average per capita of water uptake in kg/person/daily in Namibia is 1-L) / Average body weight (av. Body weight of a Namibian is 59.58) (Walpole et al., 2012).

The health risk assessment was determined using the USEPA Risk Assessment Methodology (Iqbal and Shah, 2013). This was calculated with Equation 1:

$$\text{Exp} = C_{water} \times IR \times EF \times ED/BW \times AT \quad (1)$$

*Exp*: Exposure dose via ingestion of water (mg/kg/day); average concentration of assessed metals in water (µg/L); IR = ingestion rate which is 2.2 L/day for adults and 1.8 L/day for children; Exposure Frequency (EF) = 365 days/year; Exposure Duration (ED) = 70 years for adults; and 6 years for children; Average body weight (BW) = 70 kg for adults; 15 kg for children; Averaging time (AT) = 365 days/year $\times$ 70 years for an adult; 365 days/year × 6 years for a child. For the characterization of risks, the Hazard Quotient (HQ) of the analyzed heavy metals must be determined with reference to non-carcinogenic exposure through ingestion in relation to the reference dose (R*f*D).

### *Non-carcinogenic health risks assessment*

Human health risk assessment in relation to non-carcinogenic effect due to possible consumption of water that is contaminated by heavy metal was deduced as the quotient of daily intake (mg/kg/day) of the metal with reference to ingestion toxicity reference dose (R*f*D) for the development of hazard quotient (HQ) as specified (USEPA, 2004) (Equation 2):

$$\text{HQ} = Exp/RfD \quad (2)$$

HQ is the hazard quotient through oral ingestion and R*f*D is the metallic reference dose (*µ*g/kg/day).

### *Total hazard quotient (HQ)*

To measure the overall non-carcinogenic effects caused by more than one metal, the quantity of the calculated HQ*s* by all metals through oral ingestion was articulated as hazard index (HI) as computed in Equation 3 (Iqbal and Shah, 2013):

$$\text{Hazard index equation (HI)} = \sum \text{HQ} \quad (3)$$

where HI is the hazard index through the ingestion pathway. Health Index, HI > 1 showed that exposure to the borehole water may pose possible impacts on human health (Igbal and Shah, 2013).

**Chronic daily intake (CDI)**

Chronic daily intake *(CDI)* of heavy metals via ingestion was deduced using Equation 4 (Shen et al., 2014):

$$CDI = C_{water} \times DI/BW \quad (4)$$

where DI = average daily intake of water (1.8 L/day for children; 2.2 L/day for adults); BW = body weight (15 kg for children and 70 kg for children), and Cwater = concentration of trace metal in water in (mg/kg).

***Carcinogenic health risk index (CRI)***

CRI assesses the probability of the development of carcinogenic effects, that is, the development of cancer as a result of ingestion of water samples. Equation 5 was used in expressing the carcinogenic risk (USEPA, 2004):

*Carcinogenic Health Risk Index = Estimated Daily Intake/Carcinogenic Slope Factor* (5)

For the carcinogenic slope factor of metals in mg/kg/day, R*f*D is the oral reference dose mg/L/day. A limit of $1.0\times10^{-6}$ to $1.0\times10^{-4}$ was anticipated as the permissible range (that is, 1 in 10,000) for carcinogenic harm over a 70-year generation (Igbal and Shah, 2013). The CRI was determined for possible indication of lifetime risk of exposure. A carcinogenicity risk value of $1.0 \times 10^{-6}$ is the upper limit of acceptability with respect to the development of cancer. Values above this range indicate a higher propensity for developing cancer (USEPA, 2016).

**Microbial analysis**

For the possible presence of microbial entities in water samples, the number of colonies in each plate was counted. Hence, the HTP, *Tc*, and *Fc* were determined. Hence, the Colony-Forming Units (cfu/ml) were deduced as:

Number of colonies × Dilution factor) / (Volume plated)

**Statistical application**

Data were subjected to descriptive and inferential statistics. The correlation coefficient was applied to establish a possible relationship or association between parameters. In addition, the Shapiro-Wilk test for normality was applied for the assessment of the normal distribution of data.

## RESULTS AND DISCUSSION

### Physico-chemical parameters

The physicochemical parameters that were assessed for the quality of water in sampled boreholes are presented in Table 1, while the results of the analysis of these parameters across the sampling periods (SP1-SP6) are shown in Table 2. The overall pH values of water samples ranged from 7.4 to 8.4 with an overall mean of 7.7±0.4. This range can be said to be within the acceptable recommended range of 6.5 to 8.5. A similar mean pH value of 7.22 and 7.21 during the dry and wet seasons, respectively was reported in a related study of groundwater quality (Fadili et al., 2022a). The pH of drinking water has been regarded as one of the most important water quality parameters given its role in water chemistry. Human health may not be compromised by elevated pH. However, the palatability of the water for drinking purposes may be affected (Muhammad et al., 2011). The measured temperature in °C of water samples also ranged between 19.0 and 24.0 with an overall mean of 21.5±2.0. This range is within the acceptable room temperature of 25°C depending on the preference of the consumer. A comparable mean temperature of 24.5°C has been reported in a related study (Gulilat et al., 2022).

Although cooler water is generally more acceptable and palatable than warmer ones, the borehole water across the communities can be deemed suitable for human consumption in this regard. However, high temperature is known to influence the rate of chemical and biological reactions since warmer temperatures promote microbial growth and may influence the taste, color, corrosion, and odor of water (Uribe-Loríо et al., 2019). Turbidity indicates the cloudiness of water due to suspended matter and precipitates. According to WHO, turbidity above 4 NTU reveals a whitish precipitate and reduces water acceptability for drinking purposes. Turbid water is of health concern due to the possible attachment of chemical and microbial contaminants. The turbidity level of analyzed water samples was in the range of 71.3 to 208.4 with an overall mean of 145.4±56.3. This range is well above the prescribed 4 NTU (WHO, 2022) and thus renders the water unsuitable for drinking purposes. This confirms the blockage of piped-water systems of the community by the powdery whitish substance. From this, the water from the boreholes undoubtedly is recommended for pretreatment before consumption. A higher groundwater turbidity range of 233.1 and 168.9 during dry and wet seasons was reported in a similar study (Gulilat et al., 2022).

The level of Electrical Conductivity (EC) obtained in the study varied from 122.1 to 137.2 µS/cm with an overall mean of 127.1±5.8 µS/cm. Electrical conductivity provides an indication of the degree of water conductivity and an indication of the concentration of inorganic components in the water. Although these values, including the overall mean, are within the permissible level of 300 µS/cm (WHO, 2022), the level of dissolved solids in water utilized for drinking purpose gives cause for concern. The range of EC obtained in this study was much lower than the range of 592 to 5032 µS/cm reported in a similar study (Fadili et al., 2022a). This high value might have been influenced by possible contribution from leachate from landfills within the study area. The level of TDS in the borehole water samples across the sampling periods ranged from 805.7 to 875.9 mg/L with an overall mean level of 832.8±24.4 mg/L. The range and overall mean concentration are higher than the prescribed level of 600 mg/L considered being ideal for drinking purposes. TDS above this level is

**Table 1.** Selected Physico-chemical parameters analyzed in the borehole water samples.

| Parameter | Unit/Scale | Analytical technique |
|---|---|---|
| pH | 0 - 14 | Portable field meter |
| Temperature | °C | Portable field meter |
| Turbidity | NTU | Portable field meter |
| EC | µS/cm | Portable field meter |
| Total Dissolved Solids | mg/L | Portable field meter |
| Heavy Metals (Zn, Cd, Cu, Pb,Fe and Mn) | mg/L | ICP-OES |
| Microbial Analysis | cfu | PCR |

PCR = Polymerase chain reaction; EC = electrical conductivity.

**Table 2.** Mean and overall mean levels of selected physicochemical parameters in borehole water samples.

| SP | Parameters | | | | TDS (mg/L) |
|---|---|---|---|---|---|
| | pH | Temp (°C) | Turbidity (NTU) | EC (µS/cm) | |
| SP1 | 7.5 | 20.3 | 175.0 | 130.7 | 875.9 |
| SP2 | 7.4 | 20.0 | 208.4 | 122.7 | 821.9 |
| SP3 | 7.6 | 19.0 | 174.0 | 124.5 | 834.6 |
| SP4 | 7.8 | 23.1 | 164.0 | 125.3 | 840.1 |
| SP5 | 8.4 | 24.0 | 79.4 | 137.2 | 805.7 |
| SP6 | 7.5 | 22.7 | 71.3 | 122.1 | 818.7 |
| $X_0$±SD | 7.7±0.4 | 21.5±2.0 | 145.4±56.3 | 127.1±5.8 | 832.8±24.4 |
| MAL | 6.5-8.5 | 25°C | 4.0 | 300 | 1000 |

SP = Sampling periods; $X_0$ = overall mean; MAL = maximum acceptable limit.

generally unpalatable with a salty taste (WHO, 2022). Although, this may not cause any adverse health effects in the short-term, however, the possibility of salt overload in sensitive individuals in the long term may occur (Hohls et al., 2002). Some elevated level 386 to 3.221 mg/L with a mean value of 1.185 mg/L during the wet season and 424 to 3.232 mg/L with a mean value of 1.199 during the dry season of TDS in drinking water has been reported (Fadili et al., 2022a).

## Concentration of heavy metals in borehole water samples

The results of the analyzed heavy metals in water samples are presented in Table 3. The normality of data obtained in this study was evaluated through the application of the Shapiro–Wilk test. The obtained $P$ value of 0.294 is > 0.05, indicating normally distributed data. The levels of Zn, Cd, Cu, Pb, Fe and Mn ranged from 0.1 to 1.8 (0.72±0.6 mg/L), 0.01, 0.01, 0.02, 0.02 to 9.2 mg/L (4.8±5.1 mg/L) and 0.1 to 19 mg/L (4.4±7.2 mg/L), respectively across the sampling periods (SP1-SP6). It is interesting to note that the level of analyzed metals, particularly Zn, Fe, and Mn were higher during SP1 and SP2 while the metallic concentrations across SP3-SP6 were fairly constant with marginal differences. This might be due to the mobilization of suspended or dissolved solids in the water aquifer as a result of higher water usage. Heavy metals have been reported to adhere to particulate matters which are later mobilized under favorable conditions of pH and other chemical factors (Han et al., 2020).

Zinc was detected in all analyzed water samples, however, the level obtained as well as the overall mean levels were lower than the permissible limit recommended for drinking (WHO, 2022) and irrigation purposes. The lower level of Zn was also obtained in a similar study (Fadili et al., 2022a). Zinc is among the metals that have been categorized as "essential" as a result of some roles played as a food supplement, particularly in sporting activities (Yang et al., 2003). However, elevated level of this metal has been reported to be toxic (Plum et al., 2010). The concentration of Cd obtained in water samples across the sampling periods was 0.01 mg/L. Cadmium is usually considered in many water contamination, toxicological, and public health studies given its toxicity and non-essentiality in human physiology even in small amounts. Cadmium has been associated with carcinogenic and endocrine-disrupting activities in humans (Pollack et al., 2011; Ali et al., 2012). The level of Cd obtained in this study was higher than the WHO drinking water permissible level and may also be unsuitable for irrigational use (Ayers and Westcot, 1985). Detection of Cd at this level gives cause for concern given its toxicity, potential for

**Table 3**. Mean and overall mean level of trace metals (mg/L) in water samples and EDI across sampling periods.

| SP | Parameter | | | | Fe | Mn |
|---|---|---|---|---|---|---|
| | Zn | Cd | Cu | Pb | | |
| SP1 | 1.8 | 0.01 | 0.01 | 0.02 | 9.2 | 19.0 |
| SP2 | 1.0 | 0.01 | 0.01 | 0.02 | 11.4 | 2.3 |
| SP3 | 0.1 | 0.01 | 0.01 | 0.02 | 0.02 | 0.1 |
| SP4 | 0.6 | 0.01 | 0.01 | 0.02 | 7.0 | 1.9 |
| SP5 | 0.4 | 0.01 | 0.01 | 0.02 | 0.6 | 1.5 |
| SP6 | 0.4 | 0.01 | 0.01 | 0.02 | 0.3 | 1.4 |
| $X_0$±SD | 0.72±0.6 | 0.01 | 0.01 | 0.02 | 4.8±5.1 | 4.4±7.2 |
| EDI (adults) | $2.6\times10^{-2}$ | $3.1\times10^{-4}$ | $3.1\times10^{-4}$ | $6.2\times10^{-4}$ | $5.6\times10^{-1}$ | $2.2\times10^{-1}$ |
| EDI (children) | $1.0\times10^{-1}$ | $1.2\times10^{-3}$ | $1.2\times10^{-3}$ | $2.4\times10^{-3}$ | $2.13\times10^{0}$ | $8.5\times10^{-1}$ |
| WHO Limit(D) | 5.0 | 0.003 | 2.0 | 0.01 | 0.3 | 0.08 |
| FAO Limit(I) | 2.0 | 0.01 | 0.2 | 5.0 | 5.0 | 0.2 |

SP = Sampling periods; $X_0$ = overall mean; EDI = estimated daily intake; SD= standard deviation; $WHO_D$ = drinking water; $FAO_I$ = Irrigation.
Source: Ayers and Westcot (1985).

bioaccumulation, and long-term health implications.

Concentrations of 0.01 and 0.02 mg/L were obtained respectively for Cu and Pb in analyzed water samples across the sampling periods. Copper (Cu) is among the metals that have been categorized as essential as a result of the role it plays in human physiology. However, toxicity at higher levels in humans has been reported (Osredkar and Sustar, 2011) including its implication in the genetic disorder of hepatic copper metabolism, also called the Wilson Disease (Aggarwal and Bhatt, 2018). The concentrations obtained in the study were generally lower than the WHO permissible limit of 2.0 mg/L in drinking water, however, long-term ingestion and bioaccumulation may result in health problems. The levels of Cu and Pb obtained in the study were also lower than the permissible limit of water used for irrigational purposes (Ayers and Westcot, 1985).

Lead (Pb) is a toxic, non-essential metal that has been implicated in several human health problems including disruption of cognitive capacity in children (Cruz et al., 2021). The level of Pb obtained in this study were higher than the permissible level for drinking purposes but generally lower for irrigation purpose. Detection of above permissible level of this metal in borehole water gives cause for concern given its noxious nature and health effects on humans. On the contrary, however, the concentration of Cu and Pb in groundwater reported in a related study was found to be higher than the permissible level (Dogra et al., 2023).

The level of iron (Fe) and manganese (Mn) in the analyzed samples varied from 0.02 to 11.4 mg/L (4.8±5.1 mg/L) and 0.1 to 19.0 mg/L (4.4±7.2 mg/L), respectively. The mean and overall mean levels of Fe obtained across the sampling periods, except for SP3 (0.02 mg/L) were generally higher than the permissible level for human consumption while some mean values recorded at SP1, SP2, and SP4 were found to be above the limit for irrigational purpose (Ayers and Westcot, 1985). The incidence of higher levels of Fe in drinking water has also been reported in a similar study (Gulilat et al., 2022; Dogra et al., 2023). High level of Fe in water is aesthetically undesirable and impacts the color and taste of the water. Possible sources could be a result of release from groundwater bedrock and suspension at the favorable condition of lower pH. It might also be due to possible leaching from waste disposed metals and storm runoff. It is not uncommon to find litters of metallic and other waste within the community. All the mean and overall mean levels of Mn obtained in analyzed water samples were found to be higher than the prescribed permissible level for drinking purposes and also higher for irrigational use except for the value recorded at SP3. Risk analysis of groundwater consumption reported elevated level of Mn in a similar study that was conducted in Pakistan (Shahzad et al., 2022). Consumption of water laden with high levels of Mn can lead to an increased risk of neurological disorders. Notwithstanding the essentiality classification of Mn in humans, excess amount has been linked to brain, liver, and kidney damage in developing fetuses (Markiv et al., 2023).

## Microbial entities

The results of microbial entities in analyzed borehole water samples are presented in Table 4. Analysis of pathogenic organisms in drinking water is usually carried out due to the rapidity at which ill-health, aggravation therefrom and possible fatality may occur, hence, its public health importance. HPC and Tc were detected in water samples across the sampling periods except at SP6. Although HPC is not directly linked to human ill-health, high levels may

**Table 4.** Mean level of microbial entities analyzed in water samples across the sampling periods.

| SP | Microbial entities | | |
|---|---|---|---|
| | **HPC** | ***Tc*** | ***Fc*** |
| SP1 | 1083 | 3.8 | ND |
| SP2 | 3 | 319 | ND |
| SP3 | 652.4 | 14.4 | 0.7 |
| SP4 | 1045 | 5 | ND |
| SP5 | 986.8 | 75.5 | 5.6 |
| SP6 | ND | ND | ND |
| WHO limits | NG | 0 | 0 |

NA = No guideline; ND= not detected.

however affect the aesthetic quality of water, an indication of the presence of nutrients and biofilms (Bartman et al., 2013). Detection of HPC values of 1083, 1045, and 986.8 at SP1, SP4, and SP5, respectively gives cause for concern. Other studies have reported high level (>500 cfu/ml) of HPC in desalinated household water (Yari et al., 2018) and groundwater (De Giglio et al., 2016).

Tc was detected at all sampling points with the exception of SP6. Although, detection does not necessarily indicate the onset of illness; however, it reveals the presence of harmful pathogens in the water system. Zero total coliform colonies/100 ml of water has been recommended.

*Fc* however, was detected during SP3 and SP5. According to WHO, no water intended or designated for human consumption should contain no pathogenic entity per 100 ml. However, it is important to note that *Fc* was detected only at a single sampling site. Notwithstanding, the presence of *Fc* in the borehole water sample is quite worrisome given its effects on human health, particularly in children. A similar study of the microbiological investigation of groundwater quality in Spain reported 18.12% fecal contamination out of 154 sampled wells (Suárez-Varela et al., 2014).

Consumption of drinking water that is contaminated with *Fc* may lead to incidences of diarrhea, nausea, vomiting, cramps, and other gastrointestinal distress which could be fatal in severe cases (Wang et al., 2022). A possible source of *Fc* in the water could be from animal fecal matter since large cattle farming is a traditional and one of the major agricultural activities among community members. Generally, the detection of coliform bacteria indicated contamination by fecal matter of human or animal origin (Haramoto et al., 2018).

## Health risks of consumption of water from the boreholes

Results of potential health risks from the consumption of analyzed water samples are presented in Table 6. Zinc occurs naturally in the earth's crust; however, its background level has been tremendously increased due to anthropogenic activities. The level of metals in groundwater could generally be exacerbated by the geological formation of the prevailing area. Metallic association in water samples revealed a strong association between Zn and Cd ($r$ = 0.99). The THQ and CRI of Zn for adults are $8.6\times 10^{-4}$ and 0.3; while THQ and CRI of Zn for children are $3.3\times 10^{-3}$ and 0.49, respectively; hence, there is no harm of carcinogenic and non-carcinogenic effect on human health from drinking water from Ovitoto boreholes as these values are < 1 (Table 5).

Cadmium (Cd) is a poisonous metal with no beneficial physiological properties and has been designated as a possible carcinogen. A possible source of Cd in water samples may be associated with the use of fertilizer and improper use of wastes in the community. There was no correlation between Cd and Mn ($r$= -0.83) while there was a weak correlation between Cd and Cu (r= 0.55). The THQ and CRI of Cd obtained for adults were $6.3\times 10^{-4}$ and $6.3\times 10^{-3}$, while THQ and CRI of Cd obtained for children were $2.4\times 10^{-3}$ and 0.24, respectively. From this, there is no danger of carcinogenic and non-carcinogenic effects on human health from drinking borehole water, as these values were $< 1$.

Copper is one of the metals classified as an essential element, however, at high levels, it has been linked to the genomic syndrome known as Wilson disease at high concentration. The association between the metals in water samples showed no association between copper and other metals. The THQ and CRI of Cu for adults are $7.4\times10^{-6}$ and (Nil; Not Available), while THQ and CRI for children were $3.0\times 10^{-5}$ and (Nil); therefore, there is no non-carcinogenic harm, since these values < 1.

Pb is viewed as non-essential, contaminated metals with harmful health concerns in humans. Lead has been associated with undesirable impacts on the cardiovascular system, the Central Nervous System (CNS), as well as on the immune system. The level of Lead (Pb) was above the WHO-recommended limit at all the sampling points across the sampling periods. The level of lead might be caused by aged pipes, faucets, and plumbing. Pb quantities in

**Table 5.** Health risk assessment of analyzed heavy metals in water samples.

| SP | Parameter | | | | Fe | Mn |
|---|---|---|---|---|---|---|
| | Zn | Cd | Cu | Pb | | |
| THQ (adults) | $8.6 \times 10^{-4}$ | $6.3\times 10^{-4}$ | $7.9\times 10^{-6}$ | $4.5\times 10^{-4}$ | $8.0\times 10^{-4}$ | $9.3\times 10^{-3}$ |
| THQ (Children) | $3.3\times 10^{-3}$ | $2.4\times 10^{-3}$ | $3.0\times 10^{-5}$ | $1.7\times 10^{-3}$ | $5.0\times 10^{-3}$ | $3.5\times 10^{-2}$ |
| CRI (Adults) | 0.13 | $6.3\times 10^{-2}$ | - | $7.3\times 10^{-5}$ | - | 4.74 |
| CRI (Children) | 0.49 | 0.24 | - | $2.8\times 10^{-4}$ | - | 18.10 |

THQ = Targeted hazard quotient; CRI = carcinogenic risk index.

**Table 6**. Results of the correlation co-efficient of heavy metals in the water samples.

| Metal | Zn | Cd | Cu | Pb | Fe | Mn |
|---|---|---|---|---|---|---|
| Zn | 1 | | | | | |
| Cd | 0.9998 | 1 | | | | |
| Cu | 0.5077 | 0.5580 | 1 | | | |
| Pb | 0.5279 | -0.4713 | -0.4351 | 1 | | |
| Fe | 0.9999 | -0.4763 | 0.5417 | -0.4532 | 1 | |
| Mn | 0.9920 | -0.8350 | -0.5432 | 0.5642 | -0.4325 | 1 |

borehole water are similar to quantities observed for Cu whilst there was no association with other analyzed heavy metals. The THQ and CRI of Pb for adults were $4.5\times 10^{-4}$ and $7.3\times 10^{-5}$, while THQ and CRI of Pb for children were $1.7\times 10^{-3}$ and $2.8\times 10^{-4}$; hence, there is no risk of carcinogenic and non-carcinogenic effect on human health from the drinking of Ovitoto borehole water, as these values are < 1.

A high concentration of Fe in water could make the water aesthetically undesirable due to coloration impact on the medium. There was no correlation between Fe and other analyzed metals in water samples. The THQ and CRI of Fe for adults are $8.0 \times 10^{-4}$ and (Nil); while THQ and CRI for Cd for children is $5.0 \times 10^{-3}$ and (Nil); therefore, there is no risk of non-carcinogenic, as this value $< 1$. Excess Mn in water can lead to an increased risk of susceptibility to neurological disorders. Consuming excess manganese over prolonged exposure has also been associated with Parkinson-like syndrome referred to as manganism. There was no correlation of Mn with other analyzed metals. The THQ and CRI of Mn for adults were $9.3 \times 10^{-3}$ and 4.7, while THQ and CRI of Mn for children were $3.5\times 10^{-2}$ and 18.1; hence, there is no harm of non-carcinogenic effect on human health from drinking Ovitoto borehole water in both adults and children. A similar study of groundwater quality investigation in Ethiopia revealed higher HQ values of 1.1108 and 1.5537 for adults and children, respectively, hence unacceptable non-carcinogenic risk (Gulilat et al., 2022).

However, there is a risk of a carcinogenic effect on human health from the consumption of borehole water in both adults and children, since these values are $> 1$. A similar cause for concern was expressed by Gyimah et al. (2023) where Cd (CRI: $6.1 \times 10^{-4}$) contributed most to the total carcinogenic risk with adults being more vulnerable to the cancer risk than children.

## Conclusion

Results of the quality and health risk assessment of borehole water samples from the Ovitoto municipal community revealed what can be regarded as an isolated yet significant cause of concern regarding the contamination of water samples. Most of the analyzed physical parameters were within the permissible level except for TDS which could have been influenced by the geological characteristics of the area. However, a significant human health threat from TDS is not expected. The detection of some metals (Cd, Pb, Fe, and Mn) above the WHO permissible limits for drinking and irrigational purposes is quite worrisome given possible bioaccumulation and long-term health implications. The detection of coliform bacteria in some of the water samples gives cause for concern since drinking water is expected to be of zero count. Of further concern are the carcinogenic health risks index (CRI) outlook for Mn in both adults and children. Summarily, pretreatment of water from susceptible boreholes before utilization for drinking purposes is highly recommended.

## CONFLICT OF INTERESTS

The authors have not declared any conflict of interests.

## ACKNOWLEDGEMENT

The authors are grateful for the assistance provided by the Namibia Water Corporation towards the analysis of water samples.

## REFERENCES

Ahamad A, Kumar A, Kushawaha J, Singh P, Mishra PK (2018). Geochemical assessment of groundwater quality for its suitability for drinking and irrigation purpose in rural areas of Sant Ravidas Nagar (Bhadohi), Uttar Pradesh. Geology, Ecology and Landscape 2(2):127-136.

Ali I, Damdimopoulou P, Stenius U, Adamsson A, Akesson A, Berglund M, Håkansson H, Halldin K (2012). Cadmium-Induced Effects on Cellular Signaling Pathways in the Liver of Transgenic Estrogen Reporter Mice. Toxicological Sciences 127(1):66-75.

Alley ER (2000). Water Quality Control Handbook, 2nd Edition. The McGraw-Hill Companies, Incorporated, New York.

Aggarwal A, Bhatt M (2018). Advances in Treatment of Wilson Disease. Tremor and Other Hyperkinetic Movements 8:252.

Ayers RS, Westcot DW (1985). Water quality for agriculture. Rome, Italy: Food and Agriculture Organization (FAO) of the United Nations.

Bartman J, Cotruvo J, Exner M, Fricker C, Glasmacher A (2013). Heterotrophic Plate Counts and Drinking-water Safety: The Significance of HPCs for Water Quality and Human Health. IWA Publishing, London 12:1.

Bexfield LM, Belitz K, Lindsey BD, Toccalino PL, Nowell LH (2021). Pesticides and Pesticide Degradates in Groundwater Used for Public Supply across the United States: Occurrence and Human-Health Context. Environmental Science and Technology 55(1):362-372.

Cobbina SJ, Duwiejuah AB, Quansah R, Obiri S, Bakobie N (2015). Comparative Assessment of Heavy Metals in Drinking Water Sources in Two Small-Scale Mining Communities in Northern Ghana. International Journal of Environmental Research and Public Health 12(9):10620-10634.

Cruz VP, Ortega RD, Esquivel DFG, Ayala TB, Pineda B, Manzo SG, Quino JM, Mora PC (2021). Cognitive Impairment Induced by Lead Exposure during Lifespan: Mechanisms of Lead Neurotoxicity. Toxics 9(23):1-30.

Daly S, Lowe J, Hornsby G, Harris A (2021). Multiple water source use in low- and middle-income countries: a systematic review. Journal of Water and Health 19(3):370-392.

De Giglio O, Barbuti G, Trerotoli P, Brigida S, Calabrese A, Di Vittorio G, Lovero G, Caggiano G, Uricchio VF, Montagna MT (2016). Microbiological and hydrogeological assessment of groundwater in southern Italy. Environ Monit Assess 188(11):638.

Dhakal N, Salinas-Rodriguez SG, Hamdani J, Abushaban A, Sawalha H, Schippers JC, Kennedy MD (2022). Is Desalination a Solution to Freshwater Scarcity in Developing Countries? Membranes 12:381.

Dogra S, Sharma K, Singh N (2023). Water quality and health risk assessment of heavy metals in groundwater of Ranbir Singh Pura tehsil of Jammu and Kashmir, India. Environmental Monitoring and Assessment 195(9):1026.

Fadili HE, Ali MB, Mahi ME, Cooray AT, Lotfi EM (2022a). A comprehensive health risk assessment and groundwater quality for irrigation and drinking purposes around municipal solid waste sanitary landfill: A case study in Morocco. Environmental Nanotechnology, Monitoring and Management 18:100698.

Fadili HE, Ali MB, Touach N, Mahi ME, Lotfi EM (2022b). Ecotoxicological and pre-remedial risk assessment of heavy metals in municipal solid wastes dumpsite impacted soil in Morocco. Environmental Nanotechnology, Monitoring and Management P 17.

Foteinis S, Masindi V (2021). Groundwater contamination in sub-Saharan Africa: Implications for groundwater protection in developing countries. Cleaner Engineering and Technology 2:100038.

Gulilat H, Gintamo B, Khan MA, Shukla RK, Mekonnen Z (2022). Determination of the Physicochemical Quality of Groundwater and its Potential Health Risk for Drinking in Oromia, Ethiopia. Environmental Health Insights P 16.

Gyimah E, Myers RA, Gbemadu, K, Osei B, Akoto O (2023). Appraising groundwater quality and the associated health risks of heavy metal contamination at Suame magazine. Scientific African, p. 21.

Halkman HBD (2014). Indicator Organisms, In: Encyclopaedia of Food Microbiology, 2nd edition (Eds: Batt CA, Tortorello ML, Academic Press, New York, USA pp.358-363.

Han G, Yang K, Zeng J (2020). Assessment and sources of heavy metals in suspended particulate matter in a tropical catchment, northeast Thailand. Journal of Cleaner Production 265:121898.

Haramoto E, Malla B, Shrestha RG, Tandukar S, Bhandari D, Inoue D, Sei K, Tanaka Y, Sherchand JB (2018). Identification of Human and Animal Faecal Contamination in Drinking Water Sources in the Kathmandu Valley, Nepal, Using Host Associated *Bacteroidales* Quantitative PCR Assays. Water 10(12):1796.

Herrero-Hernández E, Andrades MS, Álvarez-Martín A, Pose-Juan E, Rodríguez-Cruz MS, Sánchez-Martín MJ (2013). Occurrence of pesticides and some of their degradation products in waters in a Spanish wine region. Journal of Hydrology 486:234-245.

Hohls BC (2002). National Water Resource Quality Status Report: Inorganic Chemical Water Quality of Surface Water Resources in SA. The Big Picture. Report No. N/0000/REQ0801. ISBN No. 0-621-32935-5. Institute for Water Quality Studies, Department of Water Affairs and Forestry, Pretoria, South Africa. At http://www.iamb.it/incosusw/Leone.pdf

Ifeanyi OE, Nwandkor UU (2015). Bacteriological Assessment of Different Borehole Drinking Water Sources in Umuahia Metropolis. International Journal of Current Microbiology and Applied Sciences 4(5):1139-1150.

Iqbal J, Shah MH (2013) Health risk assessment of metals in surface water from freshwater source lakes Pakistan. Human and Ecological Risk Assessment: An International Journal 19(6):1530-1543.

Khaneghah AM, Saleh HN, Valipoor S, Zarei A, Yousefi M, Asghari FB, Mohammed AA, Amiri F (2020). Assessment of groundwater quality around municipal solid waste landfill by using Water Quality Index for groundwater resources and multivariate statistical technique: a case study of the landfill site, Qaem Shahr City, Iran. Environmental Geochemistry and Health 42:1305-1319.

Latlong.Info (2023). Latitude and longitude of Otjozondjupa Region of Namibia (NA). Available at: https://latlong.Info/namibia/otjozondjupa-region

Li P, Karunanidhi D, Subramani T, Srinivasamoorthy K (2021). Sources and Consequences of Groundwater Contamination. Archives of Environmental Contamination and Toxicology 80:1-10.

Markiv B, Expósito A, Ruiz-Azcona L, Santibáñez M, Fernández-Olmo I (2023). Environmental exposure to manganese and health risk assessment from personal sampling near an industrial source of airborne manganese. Environmental Research 224:115478.

Muhammad S, Shah MT, Khan S (2011). Health risk assessment of heavy metals and their source apportionment in drinking water of Kohistan region, northern Pakistan. Microchemical Journal 98(2):334-343.

Mulyadi A, Dede M, Widiawaty MA (2020). Spatial interaction of groundwater and surface topography using geographically weighted regression in built-up area. Earth and Environmental Science pp. 477.

Nagaraju A, Thejaswi A, Sreedhar Y (2016). Assessment of Groundwater Quality of Udayagiri area, Nellore District, Andhra Pradesh, South India Using Multivariate Statistical Techniques. Earth Sciences Research Journal 20(4):E1-E7.

NSA (2013). Namibia Statistics Agency. Namibia Labour Force Survey 2013 Report. Windhoek, Namibia.

Osmani M, Mali S, Hoxha B, Bekteshi L, Karamelo P, Gega N (2019). “Drinking water quality determination through the water pollution indicators, Elbasan district,” Thalassia Salentina 41:3-10.

Osredkar J, Sustar N (2011). Copper and Zinc, Biological Role and Significance of Copper/Zinc Imbalance. Journal of Clinical Toxicology S3:1-18.

Plum LM, Rink L, Haase H (2010). The Essential Toxin: Impact of Zinc on Human Health. International Journal of Environmental Research and Public Health 7(4):1342-1365.

Pollack AZ, Schisterman EF, Goldman LR, Mumford SL, Albert PS, Jones RL, Wactawski-Wende J (2011). Cadmium, Lead, and Mercury in

Relation to Reproductive Hormones and Anovulation in Premenopausal Women. Environmental Health Perspectives 119(8):1156-1161.

Shahzad B, Mughal A, Sultan K, Ashraf K, Hassan A, Qu Z, Haider FU (2022). Risk Analysis of Heavy Metals and Groundwater Quality Indices in Residential Areas: A Case Study in the Rajanpur District, Pakistan. Water 14(21):3551.

Shaikhan BA, Güven K, Bekler FM, Acer O, Güven RG, Güven K (2019). A highly inducible β-galactosidase from enterobacter sp. Journal of the Serbian Chemical Society 85(5):609-622.

Shen C, Naveedullah MZH, Yu C, Shen H, Duan D, Lou L, Chen Y (2014). Concentrations and Human Health Risk Assessment of Selected Heavy Metals in Surface Water of the Siling Reservoir Watershed in Zhejiang Province, China. Polish Journal of Environmental Studies 23(3).

Singh R (2014). Microorganism as a tool of bioremediation technology for cleaning environment: a review. Proceedings of the Int. Academy of Ecology and Environmental Science 4(1):1.

Suárez-Varela MM, Llopis-González A, Sánchez AL, Requena PM (2014). Assessment of the microbiological quality of groundwater in three regions of the Valencian Community (Spain). International Journal of Environmental Research and Public Health 11(5):5527-5540.

UNEP (2010). Water quality outlook. UNEP GEMS/Water Programme, Burlington, Ontario, L7R 4A6 Canada https://archive.worldwaterday.org/2010/downloads/water_quality_outlook.pdf

UNGA (2015-16). United Nations General Assembly. The human rights to safe drinking water and sanitation. Resolution adopted by the General Assembly 49:6. NY.

Uribe-Lorío L, Brenes-Guillén L, Hernández-Ascencio W, Mora-Amador R, González G, Ramírez-Umaña CJ, Díez B, Pedrós-Alió C (2019). The influence of temperature and pH on bacterial community composition of microbial mats in hot springs from Costa Rica. Microbiology Open 8(10):1-26.

USEPA (19892004). Risk Assessment Guidance for Superfund, Vol. 1, Human Health Evaluation Manual. Part E (supplemental guidance for dermal risk assessment), EPA/540/R/99/005. Office of Superfund Remediation and Technology Innovation, Washington, DC, USA. https://www.epa.gov/sites/default/files/2015-09/documents/part_e_final_revision_10-03-07.pdf

USEPA (2016). Risk-Based Concentration Table. United States Environmental Protection Agency. Available at: https://archive.epa.gov/region9/superfund/web/html/index-23.html

Walpole SC, Prieto-Merino D, Edwards P, Cleland J, Stevens G, Roberts I (2012). The weight of nations: an estimation of adult human biomass. BMC Public Health 12:439.

Wang T, Guangzhi X, Wei Y, Zhang Y, Chen J (2022). Fecal coliform distribution and health risk assessment in surface water in an urban-intensive catchment. Journal of Hydrology 604:127204.

World Health Organization (WHO) (2019). 1 in 3 people do not have access to safe drinking water- UNICEF, WHO, Geneva.

WHO (2022). Guidelines for drinking-water quality: fourth edition incorporating the first and second addenda. Geneva: World Health Organization. License: CC BY-NC-SA 3.0 IGO.

Yang XE, Long XX, Ni WZ, Ye ZQ, He LZ, Calvert DV, Stoffella JP (2003). Assessing Zinc Thresholds for Phytotoxicity and Potential Dietary Toxicity in Selected Vegetable Crops. Communications in Soil Science and Plant Analysis 34(9-10):1421-1434.

Yari AR, Mohammadi MJ, Geravandi S, Doosti Z, Matboo SA, Jang SA, Nazari S (2018). Assessment of microbial quality of household water output from desalination systems by the heterotrophic plate count method. Journal of Water and Health 16(6):930-937.

Ye C, Xie ZJ, Li C, Shi X, Shao Y, Qi W (2022). The global progress on the non-point source pollution research from 2012 to 2021: a bibliometric analysis. Environmental Sciences Europe 34:121.

Vol. 17(12), pp. 313-319, December 2023
DOI: 10.5897/AJEST2023.3216
Article Number: 882489F71586
ISSN: 1996-0786
Copyright ©2023
Author(s) retain the copyright of this article
http://www.academicjournals.org/AJEST

ACADEMIC JOURNALS
expand your knowledge

**African Journal of Environmental Science and Technology**

*Full Length Research Paper*

# Possible human health risk of selected heavy metals' mobility from municipal waste compost amended agricultural soil

**Wasiu Bolaji Tomori[1,2]*, Kehinde Oluwasiji Olorunfemi[1], Vincent Olanrewaju Onibon[3] and Tolulope Oyelekan Oyewunmi[1,4]**

[1]Department of Chemistry, Federal University of Technology Akure, Ondo State, Nigeria.
[2]Department of Chemistry, Nigeria Defence Academy, Kaduna, Kaduna State, Nigeria.
[3]Department of General Studies, Federal College of Agriculture, Akure, Ondo State, Nigeria.
[4]Department of Chemistry, Wayne State University-Detroit, USA.

Received 6 August, 2023; Accepted 26 October, 2023

**Use of organic compost in soil amendment in agricultural practice may tend to transfer heavy metals and can be a health concern. This study aims to investigate the possible mobilization of selected heavy metals from municipal compost amended soil. Experimental plots (250 m$^2$) were divided into four equal portions and alternate portions were amended with municipal compost and left for 5 weeks. Soil physicochemical characteristics for compost, compost amended soil, and unamended soil were obtained by standard procedures, single extraction was obtained by diethylenetriamine penta acetic acid (DTPA) protocol, and the geochemical forms were obtained by Bureau Community of Reference (BCR) sequential extraction method. The extracts were analyzed using Atomic Absorption Spectrophotometer (Buck Scientific Model 210). In this study, the amendment of soil with compost resulted in significant changes in various physico-chemical properties, with notable percentage increases: pH (16.72%), electrical conductivity (EC, 1509.63%), organic carbon (OC, 100.24%), organic matter (OM, 24.43%), organic nitrogen (ON, 24.41%), potassium (K, 1950.63%), sodium (Na, 325.03%), calcium (Ca, 67.93%), and magnesium (Mg, 112.92%). Although, the concentrations of metals were marginally altered by amendments, the study has revealed soil amendment with organic compost a potential source of heavy metals in diet.**

**Key words:** Heavy metals, sequential extraction, mobility, municipal waste compost, agricultural soil, environmental health.

## INTRODUCTION

The concept of recycling municipal waste nutrients and organic materials into agricultural farms is both practical

*Corresponding author. E-mail: wbtomori@futa.edu.ng or wbtomori@nda.edu.ng. Tel : +2348138639740.

Author(s) agree that this article remain permanently open access under the terms of the Creative Commons Attribution License 4.0 International License

and advantageous (Ahmed et al., 2019). Compost, which is a mixture of organic waste materials including decayed flora and other organic matter, serves as a valuable source of organic soil for gardeners, supplying nutrients to crops and enhancing soil structure, fertility, and productivity (USDA, 2005). This practice is essential for effective organic waste disposal, a fundamental aspect of compost production. The primary objective of soil amendments is to improve soil fertility and increase crop productivity. Municipal derived-compost is rich in organic matter, contains essential plant nutrient, cheap and available, therefore it has been an alternative soil amendment (Pergola et al., 2018).

Lack of proper sorting of municipal waste prior to composting is a major route for heavy metal contamination. Their concentration differs largely depending on their sources, composting process, and geographical location (Sharma et al., 2019). Often times, present in municipal wastes are batteries, cigarette, metal scraps, electronic parts, computer parts, cosmetics, non-essential elements, persistent organic compound and/or microorganism which can contribute toxic metals into compost; this may be detrimental to animals, plants, and man when absorbed into food chain (Iwegbue et al., 2005). Their presence in high concentration can restrict the use of compost on agricultural land and has raised serious concern about the application of composts in relation to public health safety and thus its use to grow crops destined for human consumption (Lar and Usman, 2014). The mobility and availability of heavy metals in soil are controlled by adsorption and desorption characteristics of soils. The adsorption and desorption of heavy metals have been proven to be associated with soil properties, including pH, organic matter content, cation exchange capacity (CEC), oxidation-reduction status (Eh), clay minerals, calcium carbonate, Fe, and Mn oxides (Caporale and Violante, 2016). Among these soil properties, soil pH was found to play the most important role in determining metal distribution and mobility and eventually bioavailability. There is a direct correlation between soil pH and metal retention (Zeng et al., 2011). Heavy metal in food has been found to produce terminal diseases (Onakpa et al., 2018).

Due to the potential risks associated with the use of heavy metal-contaminated compost, many countries worldwide have established specific guidelines and standards for compost application in agricultural settings (Arora and Chauhan, 2021). Garnier et al. (2006) have emphasized the significance of understanding the fractions and chemical forms of metals in amended soil, as they play a crucial role in determining their potential remobilization, phytoavailability, and environmental impact. As a result, the primary objective of this research is to investigate the remobilization potential of selected heavy metals in agricultural soil amended with organic compost derived from municipal solid waste in Akure metropolis, Nigeria.

## MATERIALS AND METHODS

### Farm description

The study farm is located within the premises of Federal University of Technology Akure, Ondo State, Nigeria. It is a plain land with short trees and shrubs, with no record of any agricultural activities. The farm has an area of 250 $m^2$ (25 × 10 m) and located on longitude N 07° 17’59.8”; latitude of E 005° 08’03.4”.

### Farm preparation and soil sampling

The experimental plot (250 $m^2$) used for the study was cleared and plough (30 cm) into 4 garden beds of 62.5 $m^2$ each. Alternate portions were amended with 3.75 × 50 kg compost fertilizer obtained from the Ondo State Waste Management Authority, Akure to give approximately 30 tonnes of compost/hectare of sandy clay loam soil recommended for vegetable farming (Pivato et al., 2014), while the other two alternate portions were left unamended (Figure 1). The study farm soil was mixed with the compost, up to a depth of 20 cm, left for 5 weeks for adequate compost-soil interaction (Setia et al., 2011) and then 5 points each were sampled from each segment; using systematic random sampling method, packed carefully into polythene bags and transported to the laboratory. In the laboratory, soil samples were mixed thoroughly, air-dried at room temperature in a dust free laboratory, disaggregated using agate mortal, sieved through 2.0 mm BS standard sieve and kept in clean polyethylene bag for analysis (Inengite et al., 2015).

### Soil analysis

#### *Determination of soil physicochemical properties*

pH and electrical conductivity were measured using the electrometry method (ASTM, 2018). Organic carbon content was determined with the Walkley-Black method (AOAC, 2009). Soil particle sizes were analyzed through the hydrometer method as described by Inengite et al. (2015). Additionally, exchangeable bases were extracted using a 1 M ammonium acetate solution, and the resulting supernatant was subjected to analysis for potassium (K) and sodium (Na) using a Flame Photometer as well as magnesium (Mg) and calcium (Ca) using an Atomic Absorption Spectrophotometer (Inengite et al., 2015).

#### *Extraction of heavy metals using diethyleneamine tetrapenta acetic acid (DTPA)*

Solutions (20 ml) of 0.005 M DTPA, 0.01 M TEA (triethanolamine), and 0.01 M $CaCl_2$ (2:1:1) were adjusted to pH 7.3 using 0.1 M HCl and added to 10 g of compost, amended, and unamended soil. The mixture was thereafter shaken for 2 h, filtered into 60 ml sample bottle and analysed using AAS for the selected heavy metals (Wei et al., 2011).

#### *Sequential extraction of heavy metals analysis using Bureau Community of Reference (BCR) method*

A three step BCR sequential extraction procedure (Fernandez-

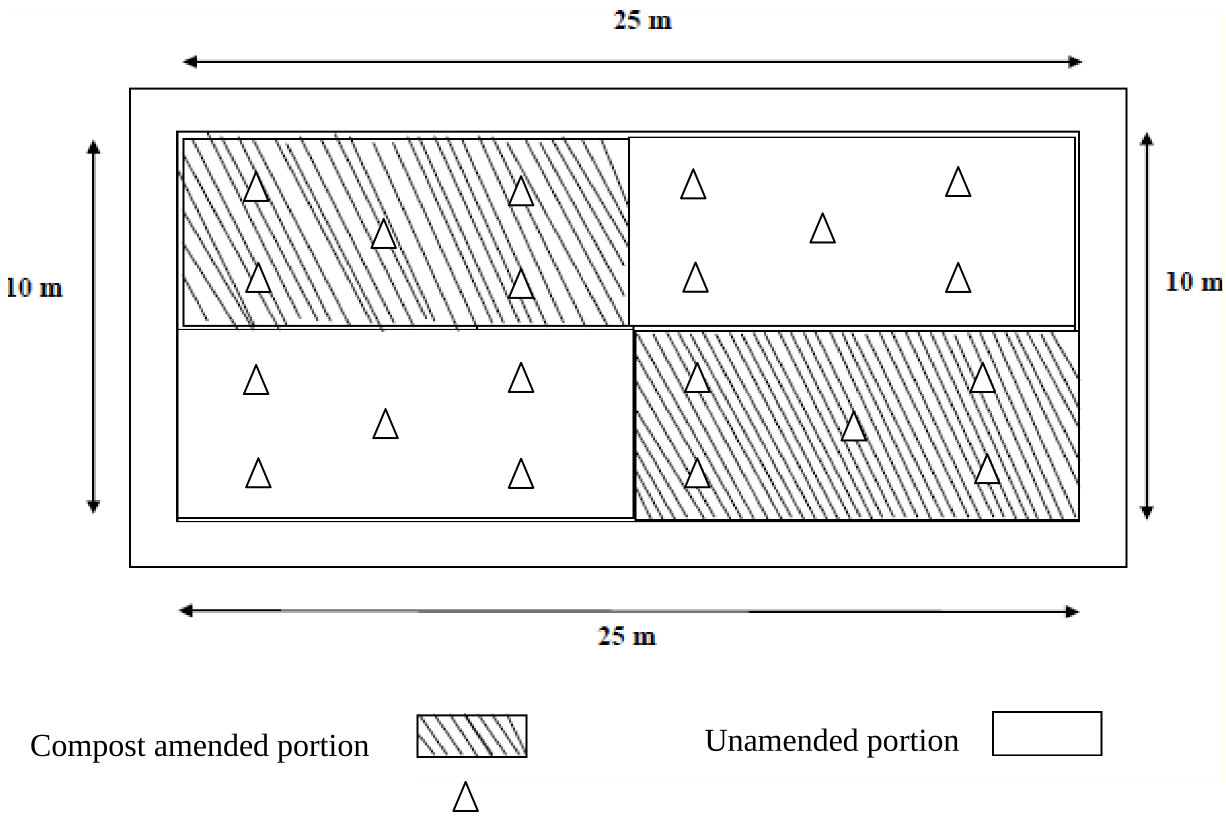


**Figure 1.** Farm sketch showing compost amended and unamended portion.

Ondono et al., 2017) was used to sequentially extract the heavy metals into their chemical form. The residue was treated with aqua regia as depicted in Figure 2.

#### Statistical analysis

Significant differences between concentrations of heavy metals in compost-amended and unamended soil as well as fraction 1 of BCR sequential extraction and DTPA single extraction were analyzed by ANOVA. Statistical significance was defined as $p < 0.05$.

## RESULTS AND DISCUSSION

Table 1 presents the characteristics of the compost (CMP), compost-amended soil (CAS), and unamended soil (UAS). The pH of unamended soil, compost amended soil, and compost ranged between 5.68 and 9.07. The pH of the unamended soil and compost-amended soil is within most plants' optimum pH of 5.5 to 7.0 whereas that of compost is a little higher. Compost application has been known to increase soil pH thereby limiting the mobility of heavy metals (Beesley et al., 2010; Fanrong et al., 2011). Electrical conductivity increases from 44.67 µS/cm in UAS to 75.17 µS/cm in compost-amended soil. Organic carbon content was 37.5 g/kg in compost, this equally translated to higher organic carbon from 25.35 g/kg in UAS to 31.55 g/kg in compost-amended soil. Compost application on unamended soil recorded a percentage increase of 32.40% in soil organic carbon. C/N ratio has a value of 20.00 for compost which is marginal after application. The concentrations of exchangeable cations are Na (28.01 g/kg), Mg (47.27 g/kg), K (147.03 g/kg), and Ca (153.49 cmol/kg) for CAS and Na (6.59 g/kg), Mg (22.20 g/kg), K (7.17 g/kg), and Ca (91.40 g/kg) for unamended soil. The possible reason for the higher concentrations of exchangeable cations and organic matter in compost-amended soil could be related to the decomposition of organic material in municipal waste to release K, Na, Ca, and Mg into the soil and makes soil less susceptible to erosion, which is in line with the work of Fageria (2009).

Compost-amended soil and unamended soil fall into similar textural class of sandy clay loam.

DTPA is regarded as a more attractive alternative to acids or bases in metal extraction processes because they can form strong metal-ligand complexes and are thus highly effective in remediating heavy metal-contaminated soils (Malathi and Stalin, 2018). DTPA on the other hand is a single extraction method and it is

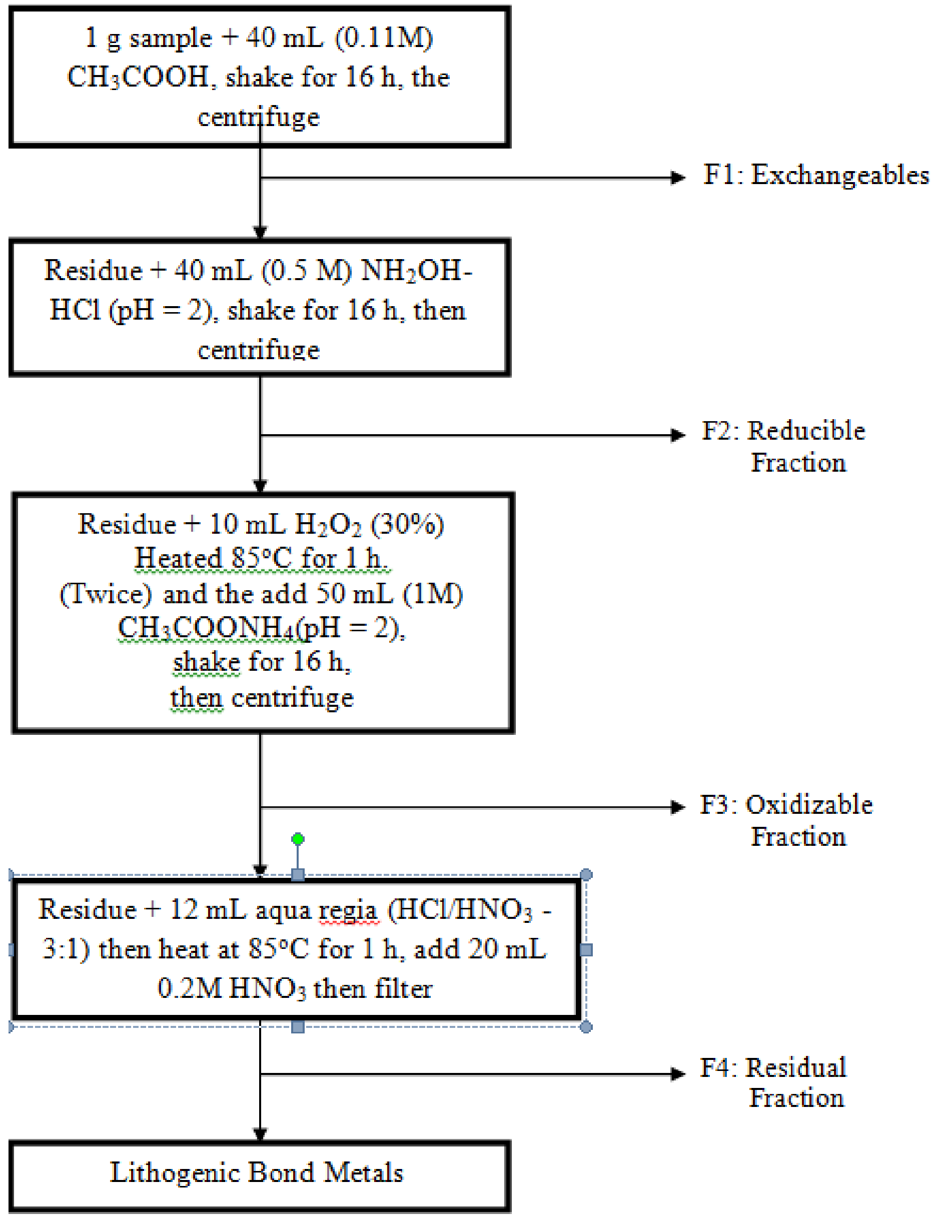


**Figure 2.** Flow chat of BCR sequential extraction method.

usually used to mimic plant nutrient uptake. The mean concentration of Fe, Cu, Zn, Pb, and Ni in UAS, CAS, and CMP using DTPA single extraction is presented in Table 2. For all metal, CMP has the highest extracted concentrations, followed by CAS. The concentration of the metals is in the following decreasing order: Fe > Zn > Cu > Ni > Pb, Fe > Zn > Ni > Cu > Pb, and Fe > Zn > Ni > Cu > Pb for UAS, CAS, and CMP, respectively. Fe had the highest concentration; next to it is Zn in UAS, CAS, and CMP while Pb is the least.

The chemical form and distribution of heavy metals in soil control the degree to which metal and their compound are mobile, extractable, and phytoavailable. Heavy metals in soluble, carbonates, and exchangeable fractions tend to be more mobile possibly by lower soil pH and changes in redox potential (Shen et al., 2022). The most mobile metals are removed in the first fractions and continue in order of decreasing mobility during sequential extraction procedures.

Typically, metals of anthropogenic input tend to reside in this phase while metals found in the residual fractions are of natural origin from the parent rock (Ratuzny et al., 2009). In Table 3, F1 and F2 fractions contain significant quantities of heavy metals which can be phytoavailable or

**Table 1.** Mean value of physico-chemical parameters for compost, compost amended and unamended soil.

| Parameter | N | CMP | CAS | UAS |
|---|---|---|---|---|
| pH | 6 | 9.07 ± 0.06[b] | 6.63 ± 0.21[b] | 5.68 ± 0.41[a] |
| EC (μScm$^{-3}$) | 6 | 3003.33 ± 6.09[c] | 75.17 ± 5.42[b] | 44.67 ± 5.65[a] |
| SOC (g/kg) | 6 | 37.50 ± 0.15[c] | 31.55 ± 0.61[b] | 25.35 ± 0.46[a] |
| ON (g/kg) | 6 | 1.88 ± 0.01[c] | 1.58 ± 0.03[b] | 1.27 ± 0.02[a] |
| C:N | 6 | 19.95 ± 0.00[a] | 19.97 ± 0.01[a] | 19.96 ± 0.02[a] |
| Na (cmol/kg) | 6 | 357.93 ± 1.72[a] | 28.01 ± 0.47[a] | 6.59 ± 1.23[a] |
| Mg (cmol/kg) | 6 | 153.52 ± 1.28[c] | 47.27 ± 1.17[b] | 22.20 ± 4.12[a] |
| K (cmol/kg) | 6 | 2652.62 ± 8.37[c] | 147.03 ± 1.10[b] | 7.17 ± 1.69[a] |
| Ca (cmol/kg) | 6 | 205.63 ± 1.31[c] | 153.49 ± 2.30[b] | 91.40 ± 1.89[a] |
| % Clay | 6 | - | 24.50 ± 1.06[a] | 22.50 ± 1.34[a] |
| % Silt | 6 | -- | 25.00 ± 1.14[b] | 18.00 ± 3.43[a] |
| % Sand | 6 | | 50.50 ± 3.31[a] | 59.50 ± 1.34[a] |

UAS: Unamended soil; CAS: compost amended soil; CMP: compost; N: number of replicates = 3. Alphabets in superscripts denote the homogenous groupings from ANOVA and Duncan Multiple Range test.

**Table 2.** Heavy metal concentration (mg/kg) in DTPA extraction protocol.

| Metal | CMP | CAS | UAS |
|---|---|---|---|
| | Mean ± SD | Mean ± SD | Mean ± SD |
| Fe | 74.73[c] ± 1.60 | 44.13[b] ± 0.53 | 33.42[a] ± 0.33 |
| Cu | 11.77[c] ± 0.62 | 5.78[b] ± 0.02 | 0.41[a] ± 0.00 |
| Zn | 13.43[c] ± 1.92 | 10.85[b] ± 0.01 | 0.83[a] ± 0.00 |
| Pb | 0.62[b] ± 0.00 | 0.19[a] ± 0.00 | 0.00 ± 0.00 |
| Ni | 12.31[c] ± 0.02 | 9.51[b] ± 0.01 | 0.30[a] ± 0.00 |

UAS: Unamended soil; CAS: compost amended soil; CMP: compost; N: number of replicates = 3. Alphabets in superscripts denote the homogenous groupings from ANOVA and Duncan Multiple Range test.

leached during changes in environmental conditions. They could pose threat to groundwater quality as well as plant absorption. Acidic environment also enhances the mobility of metal in the environment in this group; therefore, those metals found in F2 fraction are very sensitive to pH changes and could be leached at lower pH (Zheng et al., 2007).

In Table 3, the concentrations of Fe, Zn, and Ni in CMP, CAS, and UAS, as obtained by BCR extraction, exhibits the following order: F1 > F2 > F3 > Residual for Fe, F1 > Residual > F2 > F3 for Zn, and F1 > Residual > F3 > F2 for Ni. The results indicate that Fe, Zn, and Ni were released in easily mobilized forms (F1) at all stages of the sequential extraction for CMP, CAS, and UAS, consistent with the findings of Nomeda et al. (2008). This suggests that Fe, Zn, and Ni in the F1 fraction are readily available for plant uptake (Lee et al., 2015) and may have anthropogenic sources originating from the compost (Ratuzny et al., 2009). Aside from Fe, which is more abundant in the Earth's crust, sources of Ni and Zn in the environment include mining activities, combustion of coal, diesel and fuel oil, sewage and waste incineration, and tobacco smoking. These sources are commonly associated with municipal solid waste, making them potential contributors to the presence of Ni and Zn in compost.

A larger portion of Cu and Pb was found to be associated in the F4 (residual) which is the fraction more resistant to extraction. This could be that a larger portion of Cu and Pb occurs naturally in the parent material, that is, in the agricultural soil used in this study (Haroun et al., 2009). The concentration of Cu and Pb in UAS, CAS, and CMP obtained by BCR extraction follows this order: Residual > F 1 > F 2 > F 3. This result is similar to that of Li et al. (2012) who found percentages of Pb in soil fractions decreasing in the order of Residual > F 1 > F 3 > F 2. Metals contained in the crystal lattices of the minerals or residual phase are strongly bound and

**Table 3.** Heavy metal concentration (mg/kg) in compost, compost-amended soil and unamended soil in BCR Sequential Extraction.

| Metal | F1 | | | F2 | | | F3 | | | Residual | | |
|---|---|---|---|---|---|---|---|---|---|---|---|---|
| | CMP | CAS | UAS | CMP | CAS | UAS | CMP | CAS | UAS | CMP | CAS | UAS |
| Fe | 50.15$^{b}$ ± 0.04 | 46.24$^{b}$ ± 0.04 | 30.24$^{a}$ ± 0.05 | 34.10$^{a}$ ± 0.13 | 36.83$^{c}$ ± 1.35 | 36.34$^{b}$ ± 2.40 | 24.99$^{a}$ ± 1.09 | 29.75$^{a}$ ± 1.33 | 29.39$^{a}$ ± 0.52 | 10.49$^{a}$ ± 40.4 | 20.04$^{b}$ ± 2.28 | 19.26$^{b}$ ± 1.67 |
| Cu | 8.40$^{b}$ ± 0.03 | 5.98$^{b}$ ± 0.00 | 0.36$^{a}$ ± 0.00 | 2.30$^{c}$ ± 0.01 | 1.12$^{b}$ ± 0.01 | 0.04$^{a}$ ± 0.00 | 1.58$^{b}$ ± 0.00 | 1.09$^{b}$ ± 0.01 | 0.02$^{a}$ ± 0.00 | 7.16$^{b}$ ± 0.00 | 3.81$^{b}$ ± 0.01 | 0.30$^{a}$ ± 0.00 |
| Zn | 12.71$^{c}$ ± 0.07 | 8.55$^{b}$ ± 0.05 | 0.90$^{a}$ ± 0.00 | 3.17$^{b}$ ± 0.74 | 1.93$^{b}$ ± 0.07 | 0.20$^{a}$ ± 0.00 | 2.31$^{b}$ ± 0.69 | 1.31$^{b}$ ± 0.08 | 0.17$^{a}$ ± 0.05 | 5.91$^{c}$ ± 0.12 | 2.76$^{b}$ ± 0.02 | 0.74$^{a}$ ± 0.05 |
| Pb | 0.31$^{b}$ ± 0.00 | 0.12$^{b}$ ± 0.00 | 0.00$^{b}$ ± 0.00 | 0.002$^{a}$ ± 0.00 | 0.01$^{a}$ ± 0.00 | 0.00$^{a}$ ± 0.00 | 0.03$^{a}$ ± 0.00 | 0.01$^{a}$ ± 0.00 | 0.00$^{a}$ ± 0.00 | 0.42$^{b}$ ± 0.00 | 0.14$^{b}$ ± 0.00 | 0.00$^{a}$ ± 0.00 |
| Ni | 9.20$^{b}$ ± 0.00 | 7.10$^{b}$ ± 0.00 | 0.21$^{b}$ ± 0.00 | 0.50$^{b}$ ± 0.00 | 0.20$^{b}$ ± 0.00 | 0.04$^{a}$ ± 0.00 | 0.80$^{b}$ ± 0.00 | 0.70$^{b}$ ± 0.00 | 0.05$^{a}$ ± 0.00 | 4.94$^{c}$ ± 0.20 | 3.11$^{b}$ ± 0.20 | 0.45a ± 0.01 |

F1: Soil water + Carbonates + Exchangeables, F2: Iron/Manganese oxyhydroxides, F3: Organic matter + Sulphides, Residual: Total digestion (Remaining + silicate bound metals). Alphabets in superscripts denote the homogenous groupings from ANOVA and Duncan Multiple Range test.

consequently unavailable to the plants (Chao et al., 2007; Zhou et al., 2007). Despite this observation, their extraction in F1 fractions is the second largest and could indicate a mixed origin for these metals (that is, both anthropogenic and lithogenic).

Generally, for all metal under study, CMP exhibits the highest concentration of Fe, Cu, Zn, Pb, and Ni followed by CAS and then UAS. This is an indication that compost rich in heavy metal contamination may hold the possibility of metal transferring into soil and eventually to plant. This study has demonstrated these findings due to the relatively high heavy metal content in the compost and its potential remobilization in amended agricultural soil. It is worth noting that, although the levels of metals observed in CAS were below the permissible limits set by the WHO (2014) and the allowable metal values for compost in the USA (biosolids) and EU (Brinton, 2000).

The mean concentration of Zn, Pb, and Ni in DTPA single extraction method was higher than F1 of BCR sequential extraction method in UAS, CAS, and CMP. The same was also observed for Fe and Cu in UAS and CMP with the exemption of CAS; where the concentration of Fe and Cu in F1 of BCR sequential extraction method was higher than DTPA single extraction method. The results obtained agree with the observation of McLaughlin et al. (2000) that DTPA may over-estimate plant-available metals. F1 fraction of the BCR sequential extraction method is the sum of the exchangeable and carbonate fractions and the selected heavy metals contribute significantly to this fraction. This fraction is bioavailable and can easily be leached during changes in environmental conditions. They therefore, pose threat to groundwater quality and plant absorption.

## Conclusion

Municipally derived compost can offer cost-effective and readily available options, being rich in organic matter and essential nutrients. Amending soil with compost brings significant alterations to its physico-chemical properties and, to a lesser extent, the heavy metal content, including their distribution within the compost-amended soil. It is important to note that adding compost to soil leads to elevated concentrations of heavy metals in all BCR fractions. However, the behavior and chemistry of these metals may be significantly influenced by soil mineralogy. The application of compost has resulted in increased concentrations of Fe, Cu, Zn, Pb, and Ni across all fractions. Notably, the mobility of Fe, Cu, Zn, and Ni has increased, and they are predominantly found in the more available fractions, specifically F1 (water-soluble, exchangeable, and carbonates). The use of composted materials as organic fertilizer for soil amendment in vegetable gardens could potentially lead to metal pollution in backyard vegetable farming. As such, it is strongly recommended that the composting process should include rigorous sorting and the application of compost should be considered only when essential.

## CONFLICT OF INTERESTS

The authors have not declared any conflict of interests.

## ACKNOWLEDGEMENT

The authors thank the Federal University of Technology, Akure, Nigeria for the opportunity to use their facilities in the course of the study.

**REFERENCES**

Association of Official Analytical Chemists (AOAC) (2009). Official Method of Analysis, 25th Edition, Association of Official Analytical Chemists, Washington DC, USA. P 98.

Ahmed M, Ahmad S, Hassan F, Qadir G, Hayat R, Shaheen FA, Raza MA (2019). Innovative Processes and Technologies for Nutrient Recovery from Wastes: A Comprehensive Review. Sustainability 11(18):4938.

Arora NK, Chauhan R (2021). Heavy metal toxicity and sustainable interventions for their decontamination. Environmental Sustainability 4:1-3.

ASTM (2018). Standard Test Methods for pH of Water, ASTM-D1293-18. Available at: https://www.astm.org/d1293-18.html

Beesley LE, Jiménez M, Gomez-Eyles JL (2010). Effects of Biochar and Greenwaste Compost Amendments on Mobility, Bioavailability and Toxicity of Inorganic and Organic Contaminants in a Multi-Element Polluted Soil. Environmental Pollution 158:2282-2287.

Brinton WF (2000). Compost Quality Standards and Guidelines. Final Report by Woods End Research Laboratory, Inc to New York State Association of Recyclers, USA 42 p.

Caporale AG, Violante A (2016). Chemical Processes Affecting the Mobility of Heavy Metals and Metalloids in Soil Environments. Current Pollution Reports 2:15-27.

Chao W, Xiao-Chen L, Li-Min Z, Pei-Fang W, Zhi-Yong G (2007). Pb, Cu, Zn and Ni concentrations in vegetables in relation to their extractable fractions in soils in suburban areas of Nanjing, China. Polish Journal of Environmental Studies 16:199-207.

Fageria NK (2009). The Use of Nutrient in Crop Plants. Taylor and Francis group, CRC Press, New York, USA. pp. 32-136.

Fanrong Z, Shafaqat A, Haitao Z, Younan O, Boyin Q, Feibo W, Guoping Z (2011). The Influence of pH and Organic Matter Content in Paddy Soil on Heavy Metal Availability and Their Uptake by Rice Plants. Environmental Pollution 159(1):84-91.

Fernandez-Ondono E, Bacchetta G, Lallena AM, Navarro FB, Ortiz I, Jiménez MN (2017.) Use of BCR sequential extraction procedures for soils and plant metal transfer predictions in contaminated mine tailings in Sardinia. Journal of Geochemical Exploration 172:133-141.

Garnier J, Quantin C, Martins ES, Becquer T (2006). Solid Speciation and Availability of Chromium in Ultramafic Soils from Niquelandia. Brazil. Journal of Geochemical Exploration 88:206-209.

Inengite AK, Abasi CY, Walter C (2015). Application of Pollution Indices for the Assessment of Heavy Metal Pollution in Flood Impacted Soil. International Resource Journal of Pure and Applied Chemistry 8(3):175-189.

Iwegbue CMA, Nwajei GE, Osakwe SA (2005). Recycling Waste in Agriculture: Efficacy of Composting in Ameliorating Trace Metal Availability and Soil Borne Pathogens. European Journal of Science and Research 11(3):572-577.

Lar AU, Usman S (2014). Environmental Risk Assessment of Heavy Metals Content of Municipal Solid Waste used as Organic Fertilizer in Vegetable Gardens on the Jos Plateau, Nigeria. American Journal of Environmental Protection 3(6-2):1-13.

Lee PK, Choi BY, Kang MJ (2015). Assessment of mobility and bio-availability of heavy metals in dry depositions of Asian dust and implications for environmental risk. Chemosphere 119:1411-1421.

Malathi P, Stalin P (2018). Evaluation of AB - DTPA Extractant for Multinutrients Extraction in Soils. International Journal of Current Microbiology and Applied Science 7(03):1192-1205.

McLaughlin MJ, Zarcinas BA, Stevens DP, Cook N (2000). Soil Testing for Heavy Metals. Communications in Soil Science and Plant Analysis 31:1661-1700.

Nomeda S, Valdas P, Chen Shen-Yi, Lin Jih-Gaw (2008). Variations of metal distribution in sewage sludge composting. Waste Management 28:1637-1644.

Onakpa M, Anoka N, Ogbureke K (2018). A Review of Heavy Metal Contamination of Food Crops in Nigeria. Annals of Global Health 84:488.

Pergola M, Persiani A, Palese AM, Meo VD, Pastore V, D'Adamo C, Celano G (2018). Composting: The Way for a Sustainable Agriculture. Applied Soil Ecology 123:744-750.

Pivato A, Raga R, Vanin S, Rossi M (2014). Assessment of Compost Quality for Its Environmentally Safe use by Means of an Ecotoxicological Test on a Soil Organism. Journal of Material Cycles and Waste Management 16:763-774.

Ratuzny T, Gong Z, Wilke BM (2009). Total Concentrations and Speciation of Heavy Metals in Soils of the Shenyang Zhangshi Irrigation Area, China. Environmental Monitoring and Assessment 156:171-180.

Setia R, Marschner P, Baldock J, Chittleborough D, Verma V (2011). Relationship between Carbon-Dioxide Emission and Soil Properties in Salt Affected Landscape. Soil Biology and Biochemistry 43:667-674.

Sharma B, Vaish B, Monika, Singh UK, Singh P, Singh RP (2019). Recycling of Organic Wastes in Agriculture: An Environmental Perspective. International Journal of Environmental Research 13:409-429.

Shen Q, Xiang J, Zhang M (2022). Distribution and Chemical Speciation of Heavy Metals in Various Size Fractions of Aggregates from Zonal Soils. International Journal of Environmental Analytical Chemistry 102(16):4272-4287.

USDA (2005). U.S. Department of Agriculture, Agricultural Research Service. USDA National Nutrient Database of Standard Reference, Release 18:43-47.

Wei J, Tao T, Zhiming L (2011). Removal of Heavy Metal from Contaminated Soil with Chelating Agents. Open Journal of Soil Science 1:70-76.

Zeng F, Ali S, Zhang H, Ouyang Y, Qiu B, Wu F, Zhang G (2011). The influence of pH and organic matter content in paddy soil on heavy metal availability and their uptake by rice plants. Environmental Pollution 159(1):84-91.

Zheng GD, Chen TB, Gao D, Luo W (2007). Stabilization of Nickel and Chromium in Sewage Sludge during Aerobic Composting. Journal of Hazardous Materials 142:216-221.

Zhou JM, Dang Z, Cai MF, Liu CQ (2007). Soil Heavy Metal Pollution Around the Dabaoshan Mine, Guangdong Province, China. Pedosphere 17(5):588-594.

Vol. 17(12), pp. 320-331, December 2023
DOI: 10.5897/AJEST2023.3236
Article Number: 1DC12EB71616
ISSN: 1996-0786
Copyright ©2023
Author(s) retain the copyright of this article
http://www.academicjournals.org/AJEST

**African Journal of Environmental Science and Technology**

*Full Length Research Paper*

# Geospatial assessment of land surface temperature in Owo Forest Reserve Area, Ondo State Nigeria

**Victor A. Ijaware**

Department of Surveying and Geoinformatics, School of Environmental Technology, Federal University of Technology, Akure, Ondo State, Nigeria.

Received 2 October, 2023; Accepted 6 December, 2023

**Nigeria forest reserves acts as the last succour for the entire citizenry and also have significant contributions to her economy. This study was intended at assessing the Land Surface Temperature (LST) in Owo Forest Reserve Area (FRA) with a view for sustainable forest management. The objectives set for the research includes: (i.) assessing the vegetation changes in Owo FRA, (ii.) evaluate the LST and (iii.) relate changes in vegetation cover to LST to ascertain whether the observed difference in vegetation cover have noticeable effect and contribution to LST values obtained in Owo FRA. Recorded spatial coordinates of selected points constitute the primary data while the secondary data includes: Operational Landsat Imager, Enhanced Thematic Mapper, and Thematic Mapper of different years (1991, 2002, 2014 and 2020). Specifically, thermal bands of Landsat image and Normalized Difference Vegetation Index were utilized for mapping the LST. Various data acquired was processed and predicted to 2030 using Markov chain model. The results obtained showed that dense and moderate vegetation has been decreasing while non vegetation and sparse vegetation also increased for the period of studies. Again, the results garnered from 1991 to 2020 revealed that areas with vegetation (Dense, moderate and sparse) had low LST values as the forecast LST for the year 2030 are in the purview of 31.33°C(minimum) and 38.29°C (maximum). The research recommends significant increase in the rate of tree planting and preserving green areas to mitigate upsurge of LST while upholding the tenacity of laws guiding illegal logging.**

**Key words:** Normalized difference vegetation index, landsat imagery, Markov-chain model analysis, Idrisi Selva.

## INTRODUCTION

In today's world, Land Surface Temperature (LST) is a trending issue due to its effects on climate and environmental change at the three-tier level of evaluation, namely: neighborhood, locality, and international levels. The resultant effect of LST originates from the unimaginable rate of urbanization and its corresponding

E-mail: vaijaware@futa.edu.ng.

Author(s) agree that this article remain permanently open access under the terms of the Creative Commons Attribution License 4.0 International License

excessive land conversion (Balew and Korme, 2020). LST is the hotness of the Earth's surface as determined by radiative detectors. Without knowledge about LST, scientific investigations about the effects of climate change on the environment, geophysical/biophysical factors, surface energy equilibrium, and international agricultural practices would have been impossible.

However, according to Crago and Qualls (2014), the function of LST is significant in many areas of geosciences, such as Earth's net radiation allocation, providing robust information about greenhouse effects, and maintaining equilibrium between crops and vegetation. The rate and timing of plant growth, according to the European Space Agency (2021), are influenced by LST, as mechanized farmers use the world's weathercast maps to evaluate water requirements for their crops during the summer, in line with the National Aeronautical Space Agency (2008). It also helps in controlling pests and crop diseases that could overtake the fields.

Furthermore, attitudes towards land use and land cover (LULC) will either create an eco-friendly environment or otherwise. This is why Feddema et al. (2005) opined that LST is the most important environmental parameter that can assist in determining the equilibrium of energy and matter exchange in the space separating the Earth's surface and the atmosphere.

Some identified challenges in the Forest Reserve Area (FRA) include: (i) the status of the vegetation cover in the forest reserve has not been determined over the years, (ii) the effect of exploitation of economic trees by wood loggers is not known, (iii) the perceived encroachment into the forest reserve by inhabitants of the camps surrounding the FRA is alarming, (iv) uneconomical utilization of forest reserves by constituted authorities, (v) the forest reserves are characterized by slow-growing trees of various species, (vi) lack of gregarious stands since most of the forest trees are lost to plant diseases and insects, (vii) absence of recent information on the forest reserve concerning vegetation change over time in the study area, and (viii) unconfirmed forest reserve depletion and the assumption that the exposed portions may likely lead to high LST values, which was the major essence for this research.

The aim of this research is to assess LST in response to vegetation cover change in Owo FRA with a view to improving afforestation and also creating sustainable forest management. The following research questions provide impetus that enables the research aim to be achieved: (i) what are the vegetation changes in Owo Forest Reserve Area? (ii) what is the status of LST in the Owo FRA? and (iii) how do changes in vegetation affect LST in the Owo FRA? By determining vegetation changes over the years using supervised classification, deriving the Normalized Difference Vegetation Index (NDVI), and generating the thermal band from satellite imageries of different years, the desired LST is obtained.

## LITERATURE REVIEW

A review of past journals for the present study reveals that Land Surface Temperature (LST) analysis has been carried out several times in the United States of America, Europe, Asia, Africa, and Nigeria. However, none has been conducted in Owo FRA. For example, Weng et al. (2004) researched the urban heat island in Indianapolis City, USA, while Tang et al. (2018), Hasnat (2021), and Jeevalakshmi et al. (2017) examined the effects of forests on temperatures in Europe and India, respectively. Mohd-Jaafar et al. (2020) examined the influence of deforestation on LST in Malaysia, while Zhi et al. (2020), Mohamadi et al. (2019), and Shatnawi and Qdais (2019) conducted studies on LST monitoring in Xigang District of Dalian City, China, Southern China, and Jordan, respectively. Furthermore, the work of El Garouani et al. (2021), How Jin Aik et al. (2021), and Ngie et al. (2016) are examples of LST research carried out in Saïss Plain, Morocco, Cameron Highland, and Durban, South Africa, consecutively. Similarly, James et al. (2020) and Agbor and Makinde (2018) are researches on LST explicitly domiciled in Bauchi and Ondo states, Nigeria. Hence, the reviewed literature confirms that remote sensing methods and geoinformatics can be used for mapping LST with respect to the environment. However, the gap that this research seeks to fill is the use of geoinformatics techniques, remote sensing methods, coupled with forest maps and Global Positioning System (GPS) to map LST and investigate changes in vegetation over time in Owo FRA, which has never been evaluated before now.

### Simulation and prediction of NDVI and LST changes

Conceptually, a special and popular technique for Land Use Land Cover modeling that shows LULCCs as a stochastic process is the Markov chain model (Weng, 2002). According to Araya and Cabral (2010), the Markovian system models the future condition of a land use system depending on the current situation. He opined that ‘Transition’ is the changing of a system from one condition to another, and ‘Transition probability’ is the probability responsible for the state transition (Equation 1).

The initial estimates of $p_{ij}$ was obtained by computing,

$$P_{ij} = N_{ij}/N_{i},\ (ij\ldots 1, 2, 3, \ldots, m) \qquad (1)$$

where $N_{ij}$ is the number of units transitioned from the condition i to state j, while $N_{i}$ is the number of units in condition i.

In order to forecast trends in land use change, the primary hypothesis of the model simulation process primarily generates a Land Use area transfer matrix and

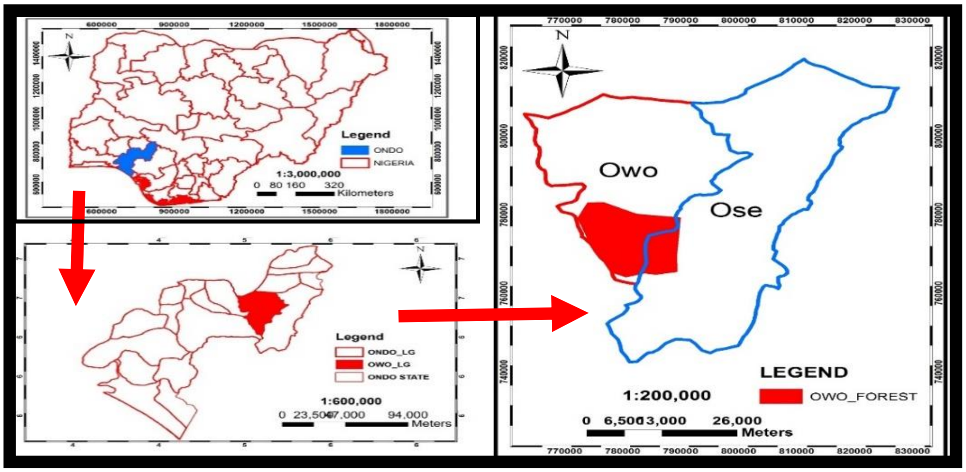


**Figure 1.** Study area map.

a probability transfer matrix (Chen et al., 2018). Assuming that the current condition is $C_t$, the Markov chain model is represented as a set of condition, C = *$C_1$, $C_2$, $C_3$, … $C_{n+}$. At each step, it moves to condition $C_j$ with a probability indicated by transition probabilities $p_{ij}$. Thus, the condition $C_{t+1}$ in the system determined by former stage $C_t$ in the Markov chain using Equation 2 (Han et al., 2015; Chen et al., 2018):

$$P_{ij} = \begin{bmatrix} P_{11} & \cdots & P_{1n} \\ \vdots & \vdots & \vdots \\ P_{n1} & \cdots & P_{nn} \end{bmatrix}$$

$$(0 \leq p_{ij} \leq 1 \; and \; \sum p_{ij} = 1 \; i, j, \ldots, n) \; C_{t+1} = p_{ij} \, x \, C_t \ldots \qquad (2)$$

where n = number of land use kinds, C= land use state, t = time frame, and $p_{ij}$= condition transition probability matrix. Essentially, the Markov chain analysis was applied in this study throughout for four time periods, viz: 1991-2002, 2002-2014, 2014-2020, and 2020-2030. As a result, the condition transition probability matrix and land use area transfer matrix for the added periods were acquired.

## MATERIALS AND METHODS

### Study area

"The Owo FRA covers an area of 241 km$^2$, approximately lying within the coordinates 7°05'N, 5°29'E; 7°03'N, 5°37'E; 6°55'N, 5°35'E; and 6°54'N, 5°32'E (Figure 1). It is situated within Owo Local Government Area (LGA) of Ondo State and extends to Ose and Idanre Local Government areas. The climate in the FRA is characterized by both wet and dry seasons, with temperatures ranging from 18 to 32°C, rarely falling below 15°C or exceeding 34°C, according to Weather Spark (2021). The average annual rainfall is reported as 1569 mm, with an average elevation of 348 m above sea level (MSL) (Meteobox, 2021). The inhabitants of Owo are primarily farmers, artisans, and lumbermen. The economy of the Owo LGA contributed significantly to the annual GDP of Ondo State.

### Data collection and processing

Data and materials adopted for this research were classified into two categorical classes, viz: primary and secondary (Figure 2). The former involves GPS coordinates obtained during the field survey exercise while the latter were derived from 30-m resolution Landsat imageries of various years (1991, 2002, 2014 and 2020) used in the research. The information of Landsat data used was in accordance to USGS (2014). Other secondary data includes: Worldview 3 image (2022), Administrative map of Ondo State and forest reserve boundary map sourced from Ondo State Ministry of Agriculture and Natural Resources, Akure.

The pre-processing stage involves the extraction of Near Infrared (NIR) and red bands from the zipped Landsat image. Significantly, the equation provided by Othman et al. (2018) was inputted into the raster calculator of the ArcGIS software to produce a raster surface showing NDVI for individual measurements while the derived NDVI images were then interpreted in line with Hashim et al. (2019). In addition, the boundary shape file (.shp) of the study area was used to clipped the derived NDVI image while LST was estimated using the thermal infrared bands in the selected Landsat images based on Single Window (SW) algorithm (Avdan and Jovanovska, 2016; Lamidi and Ijaware, 2022).

## RESULTS AND DISCUSSION

The analysis of the result is categorized into four parts, viz: the vegetation extent, the trend of vegetation categories, land surface temperature and future greenness levels, and LST using Markov chain and Cellular automata combination process.

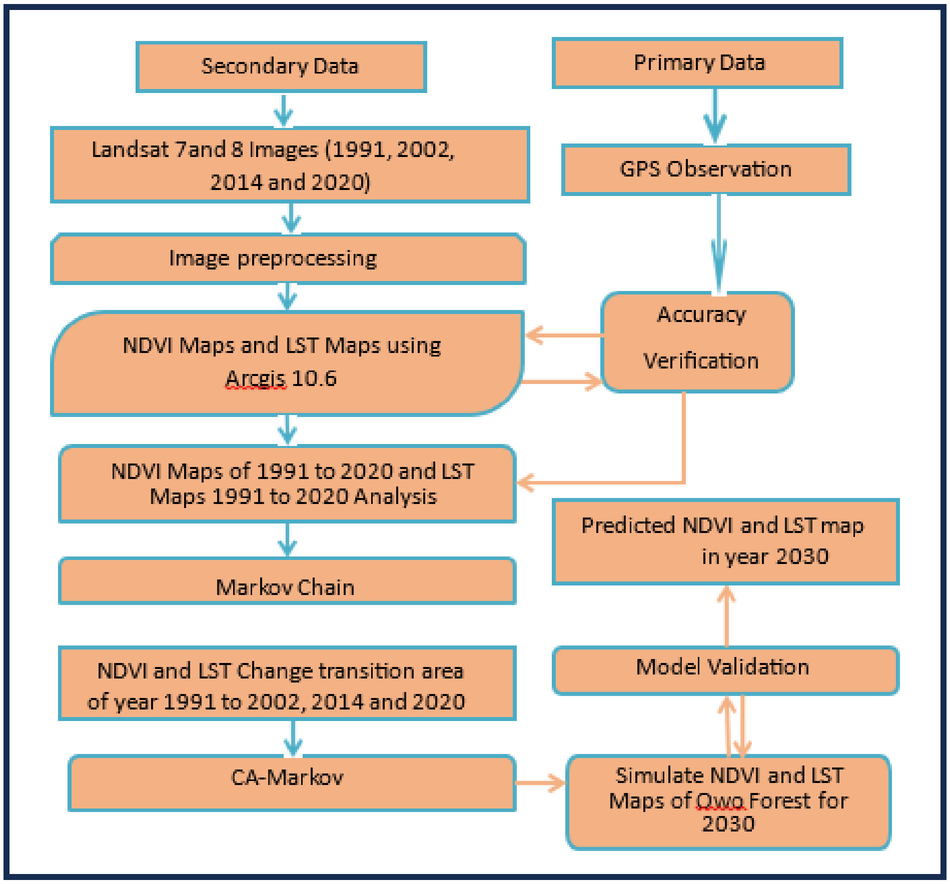


**Figure 2.** Methodology flowchart.

## Vegetation extent

The vegetation level of Owo FRA was assessed from 1991 to 2020. The vegetation levels in 1991 were classified as non-vegetation, sparse vegetation (grassland), moderate vegetation (shrub and grassland), and dense vegetation. These vegetation levels were classified based on maximum likelihood algorithm. It was observed that in the year 1991 moderate vegetation and sparse vegetation were the dominant vegetation classes while non-vegetation and dense vegetation were rarely noticeable (Table 1). The proportion of vegetation according to Figure 3a indicated that the dominant vegetation was found majorly toward the edges and central part of the FRA.

However, in the year 2002 (Figure 3b), part of sparse vegetation, which were majorly grasslands, located in the North-western part, and also towards the central part of Owo FRA changed to non-vegetation (majorly bare land), while moderate vegetation (Shrub) became the most notable categories of vegetation both in the south, southwest and southeast of Owo FRA.

In the year 2014, moderate vegetation occupied the eastern and southern part of the forest reserve, while sparse vegetation was majorly found at the middle part of the FRA. Correspondingly, non-vegetation covered small area in the central of Owo FRA. Also, the most important vegetation in the year 2020 was sparse vegetation which were found in large concentration in the entire forest reserve non-vegetation were also noticed, although dense vegetation, which are few, occurred in the southeast section of the FRA.

Significantly, throughout the year of the study, sparse vegetation consistently decreased, while moderate vegetation showed an increasing trend. However, dense vegetation did not exhibit a consistent increase. It remained undetectable for all the years from 1991 to 2014, only increasing to 0.25 km$^2$ in 2020. The rise in dense vegetation in 2020 could be attributed to the outbreak of the coronavirus pandemic, which led to a temporary halt in anthropogenic activities for about a year.

## Trend of vegetation category

The trend of each vegetation level when assessed over

**Table 1.** Extent of vegetation level in Owo FRA from 1991 to 2020.

| Name | 1991 (ha) | 2002 (ha) | 2014 (ha) | 2020 (ha) | 2030 (ha) predicted |
|---|---|---|---|---|---|
| Non-vegetation | 694.47 | 3505.91 | 1030.80 | 6850.53 | 12530.64 |
| Sparse vegetation | 8855.39 | 7290.71 | 8219.00 | 8807.73 | 6566.83 |
| Moderate vegetation | 9881.52 | 9593.12 | 9349.25 | 6296.53 | 4216.92 |
| Dense vegetation | 4892.42 | 3934.06 | 5724.76 | 2369.02 | 1002.21 |
| Total | 24323.80 | 24323.80 | 24323.80 | 24323.80 | 24323.80 |

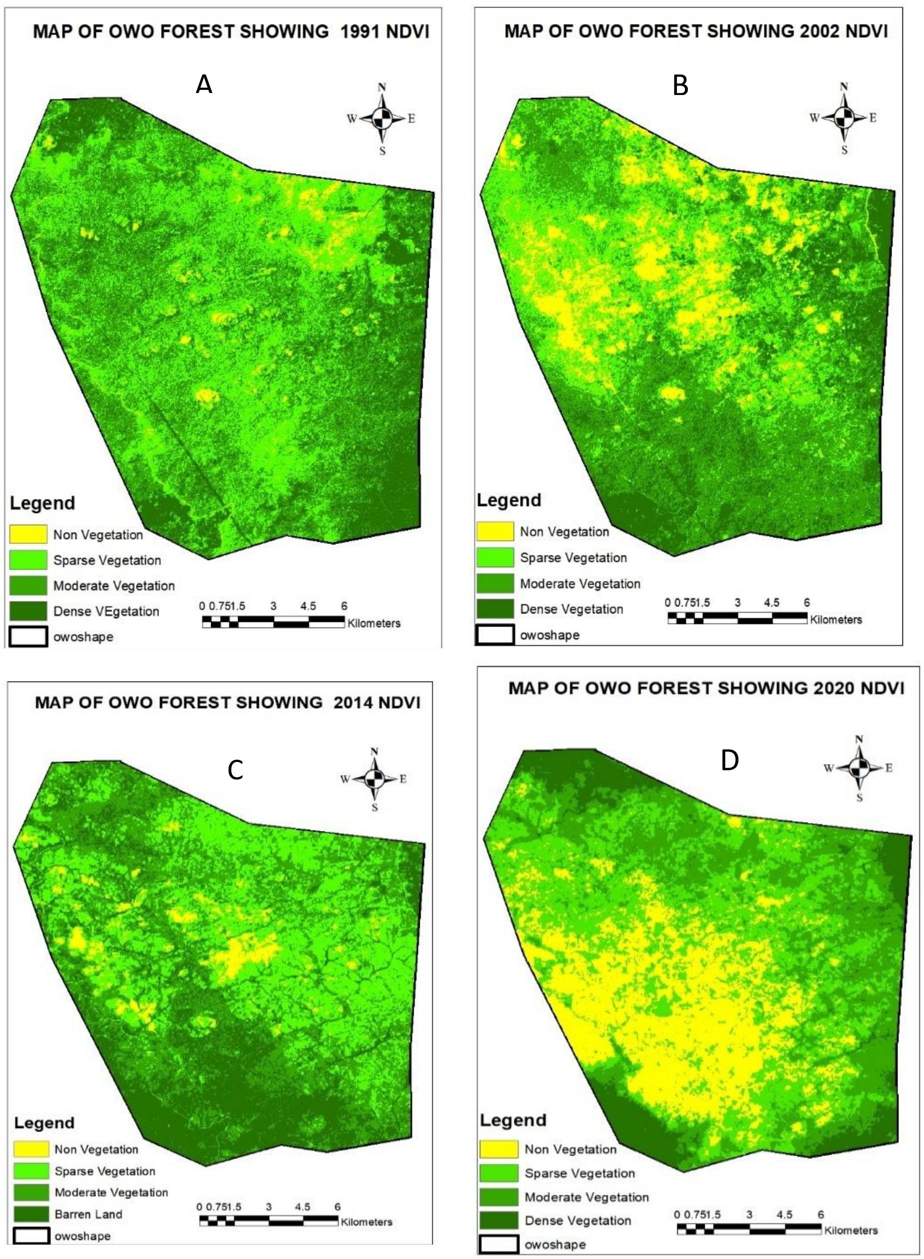


**Figure 3.** A: Map of vegetation level of Owo FRA in the year 1991; B: Map of vegetation level of Owo FRA in the year 2002; C: Map of vegetation level of Owo FRA in the year 2014; D: Map of vegetation level of Owo FRA in the year 2020.

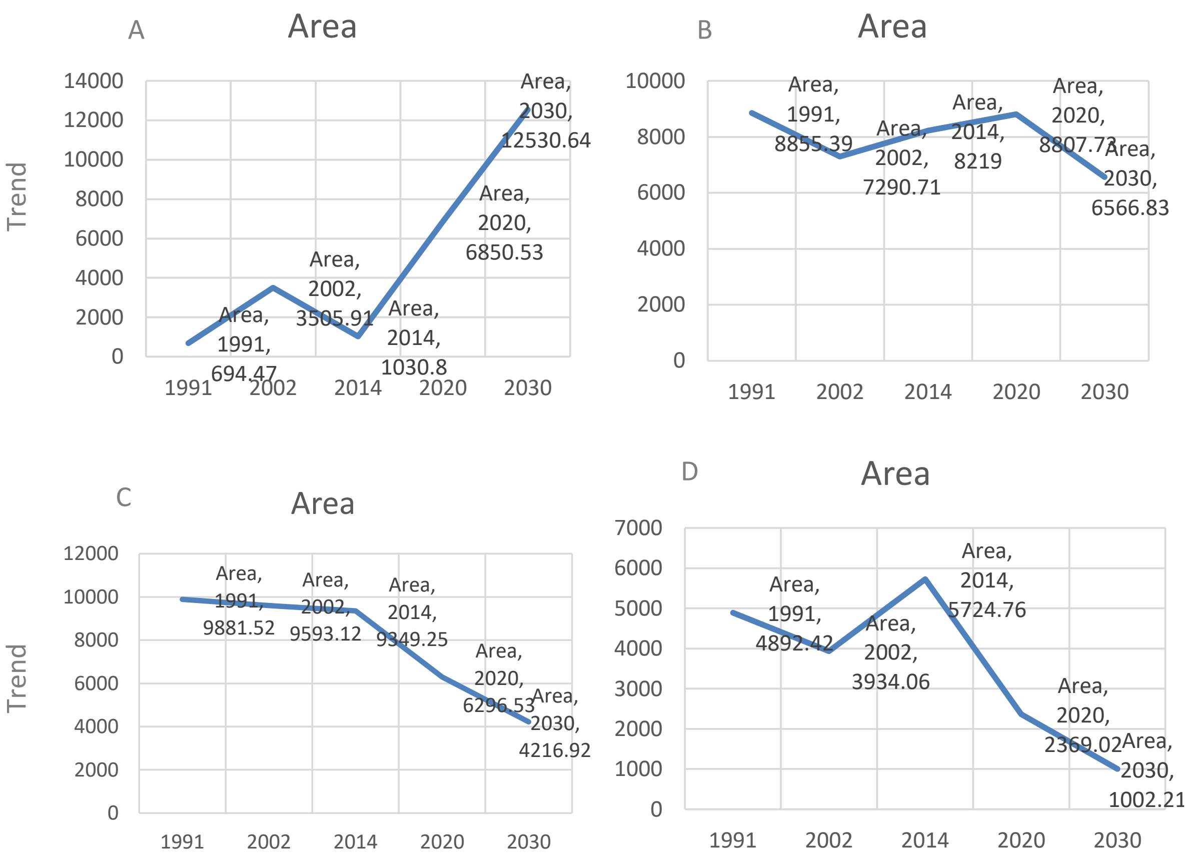


**Figure 4.** A: Trend of non-vegetation from 1991 to 2030; B: Trend of sparse vegetation from 1991 to 2030; C: Trend of moderate vegetation from 1991 to 2030; D: Trend of dense vegetation from 1991 to 2030 (Right).

the study years as presented in Figure 3a revealed that non-vegetation level increased from 694.47 to 3505.91 ha between the year 1991 and 2002 before declining to 1030.80 ha in the year 2014, and it later increased in extent to 6850.53 ha in year 2020 and was predated to 2030 with 12530.64 ha.

Declination was experienced on sparse vegetation as the extent decreased from 8855.39 ha in 1991 to 7290.71 ha in 2002, and it increase to 8219.00 and 8807.73 ha in the year 2014 and 2020 apiece as shown in Figure 4b and was predicted to 2030 with decrease to 6566.83 ha. However, moderate vegetation experienced continuous declination as the extent decreased in 1991 from 9881.52 to 6296.53 ha in the year 2020, and predicted to 4216.92 ha, in 2030 as shown in Figure 4c, Lastly, Dense Vegetation also experience declination from 4892.42 to 3934.06 ha between year 1991 and 2002, and it increased to 5724.76 ha in 2014, and later decreased to 2369.02 ha in 2020, also predicted to 1002.21 ha in 2030 as shown in Figure 4d.

Generally, the overall analysis showed that moderate and dense vegetation, which comprise shrub majorly and scattered trees have been decreasing from the beginning to the end of the research period, which signifies that the vegetation in Owo FRA has been depleting over the years due to deforestation, bush burning, agricultures activities, etc. Due to all these causes, government should enforce the law which will compel stakeholders in the forest product merchandise strict compliance and the continuous policing of the FRA against Herdsman by Amotekun corps organized and chaired by the Ondo State Governor.

## Land surface temperature (LST)

Mapping of LST at Owo FRA for the study years (1991, 2002, 2014, and 2020) yielded Figure 5a to d. Importantly, Figure 5a shows that the temperature ranged from 20.72 to 27.78°C at Owo FRA in the year 1991 and it was observed that high temperature existed in north central with small quantity while the least range temperature was observed in the northern, southern, eastern and western part of the forest reserve. Similarly,

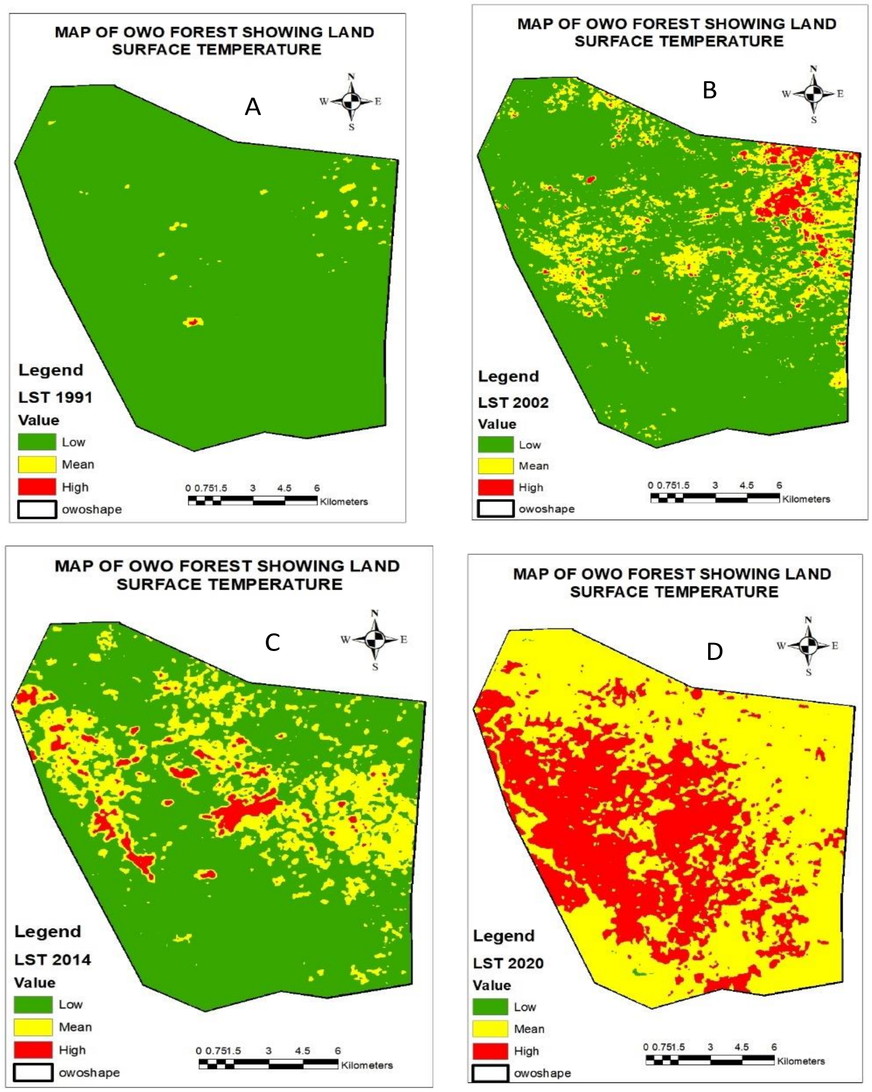


**Figure 5.** A: LST distribution in the year 1991; B: LST distribution in the year 2002; C: LST distribution in the year 2014; D: LST distribution in the year 2020.

LST values ranged between 20.27 and 30.53°C in 2002 such that, the coolest area was found in southern part which extended to north central, and northwestern part of the forest reserve while the hottest area advanced towards the northeastern part of FRA (Figure 5b).

Furthermore, in 2014, the LST values ranged from 17.43 to 30.65°C (Figure 5c) and the LST distribution showed that the least temperature was concentrated in the south, extending to the north central, while the hottest part (Places with highest LST value) domicile uniquely at the north west and middle of the forest reserve. Also, year 2020 recorded the highest range of LST values, which was from 24.38 to 34.47°C (Figure 5d) in such a way that, the southwestern and the northeastern parts of the study area were the coolest part (Places with the least LST values), while western and central part of the study area were the hottest, as they had the highest LST values. The increase in LST values were as a result of global warming that does not have boundary. The minimal, mean and the maximal values of LST were calculated to showcase LST trend for the study periods (Table 2).

From Table 2, LST values vary from one year to the other. Specifically, the minimum LST at Owo FRA was 20.72°C in 2014, which decreased to 20.27°C in 2002, and further dropped to 17.43°C in 2014, then, it escalated to 24.38°C, in 2020 and was predicted using Markov chain to 31.33°C, which was the highest of all (Figure 7a).

Also, the trend analysis of the mean LST values from

**Table 2.** Min, Mean and Max LST values from 1991 to 2020.

| Category | Years | | | | |
|---|---|---|---|---|---|
| **LST °C** | **1991 (ha)** | **2002 (ha)** | **2014 (ha)** | **2020 (ha)** | **2030 (ha) predicted** |
| Minimum | 20.72 (24098) | 20.27 (19397.18) | 17.43 (18011.83) | 24.38 (14.54) | 31.33 (0) |
| Mean | 24.25 (217.85) | 25.40 (4197.15) | 24.04 (5454.50) | 29.43 (15050.23) | 34.81 (5935.79) |
| Maximum | 27.78 (6.96) | 30.53 (729.47) | 30.65 (857.47) | 34.47 (9259.03) | 38.29 (18391.85) |

1991 to 2020 (Figure 7b) indicated that the mean LST values for the year 1991 was 24.25°C, which slightly increased to 25.40°C in 2002, but slightly decreased in 2014 to 24.04°C with an upsurge to 29.43°C in 2020, also predicted to 34.81°C in 2030. Likewise, Figure 6c shows that the maximum values of LST increased continuously from 1991 to 2020, that is, years 1991, 2002, 2014, and 2020, and the corresponding LST values were 27.78, 30.53, 30.65, and 34.47°C, respectively and also predicted using Markov chain to 38.29°C in 2030. The astronomical LST values recorded in 2020 may be as a result of climate change caused by global warming and this was in line with climate signals (2023).

## Markov chain and cellular automata combination process

The CA-Markov model is considered a robust approach because of the quantitative estimation and the spatial and temporal dynamic it has for modeling the LULC dynamic. The 1991 NDVI image of Owo Forest Priority Area used as the base image while 2020 NDVI map as the later image in Markov model to obtain the transition area matrix between 1991 and 2020 years for prediction of NDVI in 2030. Also, the image of 2014 was used as base image to obtain the transition area matrix between the years 2014 and 2020 for prediction of NDVI of the 2030. In addition to validate, model the image of 2002 as base image and the transition area matrix between 2002 and 2014 for simulation of 2020.

The result of the prediction revealed that out of all the vegetation categories found in Owo Forest Reserve, it was non-vegetation and sparse vegetation that will have significant increase in the year 2030. Table 3 is the transition matrix area between years 2014 and 2020, which was used to predict the further year of 2030. Also, Table 4 is the transition probability between years 2020 and 2030 while Table 5, is the difference between the area map of 2020 NDVI and predicted 2030 NDVI map using Idrisi Selva.

Table 6 is the transition matrix area between years 2014 and 2020 LST map, which was used to predict the further year of 2030, Table 7 is the transition probability between year 2020 and year 2030, while Table 8, is the difference between the area map of 2020 LST and predicted 2030 LST map using Idrisi Selva. Also, the outcome of the Prediction for LST values as rendered in Figure 8 shows that minimum temperature was lost in the transition, the mean and maximum temperature has increase and gain more in 2030, mean and maximal LST which fall in between 31.33 to 34.81 and 38.29°C, respectively in 2030.

Generally, the results of forecast of both NDVI and LST values at Owo FRA for the year 2030 based on the previous results showed that non-vegetation and sparse vegetation will increase, while moderate and dense vegetations will decrease in the year 2030, which implies that non-vegetation and sparse vegetation (shrub and scattered trees) will continue to increase, which is a major vegetation cover. Similarly, the minimal, mean and maximal LST will decline in year 2030, which is suspected to be as a result of the anticipated increase in non-vegetation and sparse vegetation level in the year 2030.

## Conclusion

In this study, the results revealed a significant increase in non-vegetation and sparse vegetation over the years, indicating a substantial depletion of vegetation in the Owo FRA for about three decades. The findings from 1991 to 2020 demonstrated that areas with vegetation (dense, moderate, and sparse) had the lowest LST values, suggesting that vegetation plays a role in reducing LST values. Similarly, the forecast for the year 2030 indicated that non-vegetation and sparse vegetation would continue to increase and potentially dominate the study area, while moderate and dense vegetation would decrease.

Additionally, the forecast for the year 2030 suggests an overall decline in LST in the Owo Forest Reserve, and this decrease may be attributed to the projected expansion of non-vegetation and sparse vegetation levels in that year. Furthermore, the analysis of minimum, mean, and maximum LST values in Owo FRA from 1991 to 2020 demonstrated variation from year to year. Dense vegetation consistently exhibited the lowest LST values indicating the presence of vegetation cover, while non-vegetated areas consistently showed the highest LST values over the study years. This aligns with the findings

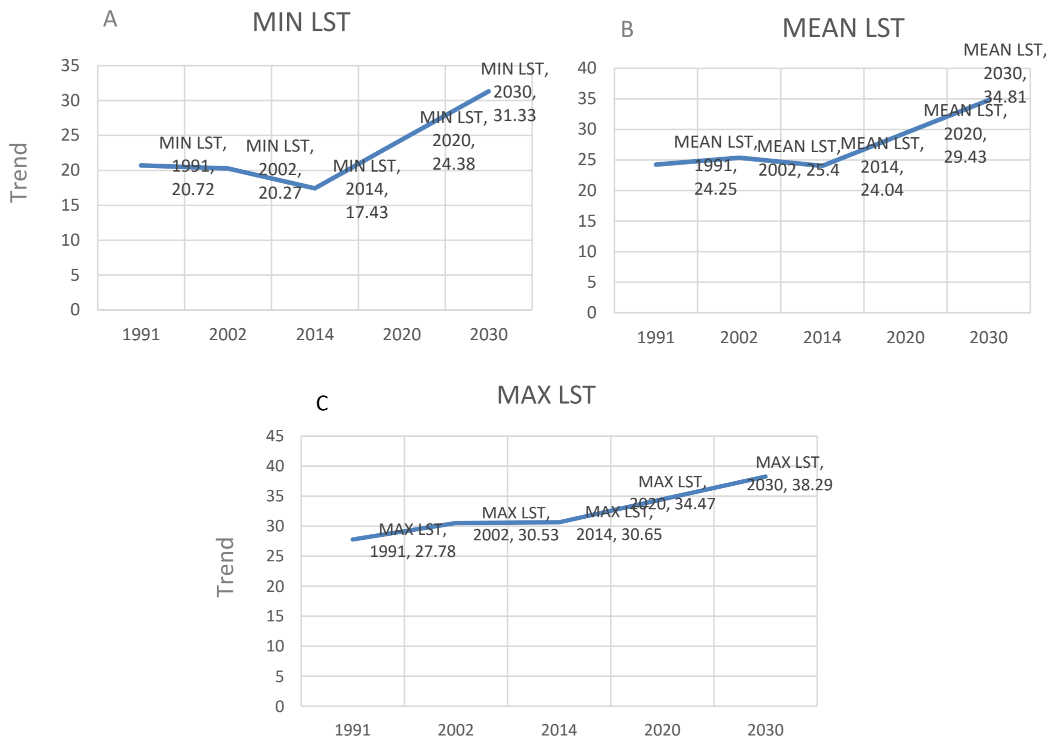


**Figure 6.** A: Trend of minimum values of LST from 1991 to 2030; B: Trend of mean values of LST from 1991 to 2030; C: Trend of maximum values of LST from 1991 to 2030.

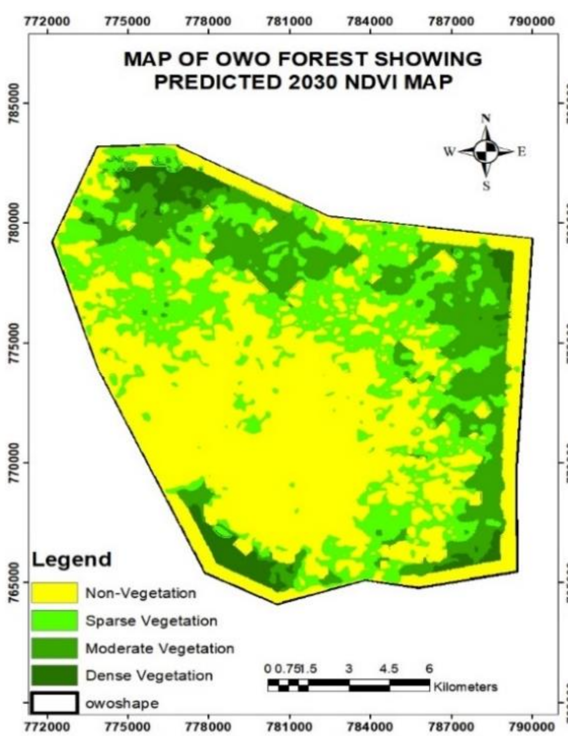


**Figure 7.** Predicted NDVI map in Owo FRA in the year 2030.

**Table 3.** Transition matrix area between years 2014 and 2020 NDVI map.

| Variable | Non-vegetation | Sparse vegetation | Moderate vegetation | Dense vegetation |
|---|---|---|---|---|
| Non-vegetation | 175495 | 10606 | 2395 | 110 |
| Sparse vegetation | 38707 | 32824 | 22696 | 3899 |
| Moderate vegetation | 26716 | 22636 | 16090 | 4708 |
| Dense vegetation | 11716 | 7190 | 5018 | 2468 |

**Table 4.** Transition probability between years 2020 and 2030 NDVI map.

| Variable | Non-vegetation | Sparse vegetation | Moderate vegetation | Dense vegetation |
|---|---|---|---|---|
| Non-vegetation | 0.9305 | 0.0562 | 0.0127 | 0.0006 |
| Sparse vegetation | 0.3945 | 0.3345 | 0.2313 | 0.0397 |
| Moderate vegetation | 0.3808 | 0.3227 | 0.2294 | 0.0671 |
| Dense vegetation | 0.4439 | 0.2724 | 0.1901 | 0.0935 |

**Table 5.** Difference between the area map of 2020 NDVI and Predicted 2030 NDVI map.

| Class | 2020 (ha) | 2030 (ha) | Changes | 2020 (%) | 2030 (%) | Change (%) |
|---|---|---|---|---|---|---|
| Non-vegetation | 6850.53 | 12530.64 | -5680.11 | 28.1639 | 51.51596 | -23.3521 |
| Sparse vegetation | 8807.73 | 6566.83 | 2240.9 | 36.21034 | 26.99755 | 9.212787 |
| Moderate vegetation | 6296.53 | 4216.92 | 2079.61 | 25.88629 | 17.3366 | 8.549692 |
| Dense vegetation | 2369.02 | 1002.21 | 1366.81 | 9.739514 | 4.120285 | 5.619229 |
| Total | 24323.80 | 24323.80 | 0 | 100 | 100 | 0 |

**Table 6.** Transition Matrix Area between year 2014 and 2020 LST map.

| Variable | Min. LST | Mean LST | Max. LST |
|---|---|---|---|
| Min LST | 18658 | 48630 | 45159 |
| Mean LST | 0 | 54498 | 113180 |
| Max LST | 0 | 7375 | 95779 |

**Table 7.** Transition Probability between year 2020 and 2030 LST map.

| Variable | Min. LST | Mean LST | Max. LST |
|---|---|---|---|
| Min. LST | 0.1659 | 0.4325 | 0.4016 |
| Mean LST | 0.0000 | 0.3250 | 0.6750 |
| Max. LST | 0.0000 | 0.0715 | 0.9285 |

of Ibrahim et al. (2016). Therefore, the results of this research establish that vegetation has a cooling effect on the LST of an area, with areas dominated by vegetation experiencing lower LST values, in line with the research of Odunuga and Badru (2015). Conclusively, the study affirms that changes in vegetation in the Owo FRA have a notable effect on LST values.

## Recommendation

The Ministries of Agriculture and Natural Resources

**Table 8.** Difference between the area map of 2020 LST and Predicted 2030 LST map.

| Class | 2020 (ha) | 2030 (ha) | Changes | 2020 (%) | 2030 (%) | Change (%) |
|---|---|---|---|---|---|---|
| Min. LST | 14.54 | 0 | 14.54 | 0.06 | 0 | 0.06 |
| Mean LST | 15050.23 | 5935.79 | 9115.4 | 61.87 | 24.4 | 37.47 |
| Max. LST | 9259.03 | 18391.85 | -9130 | 38.07 | 75.6 | -37.53 |
| Total | 24323.80 | 24323.80 | 0 | 100 | 100 | 0 |

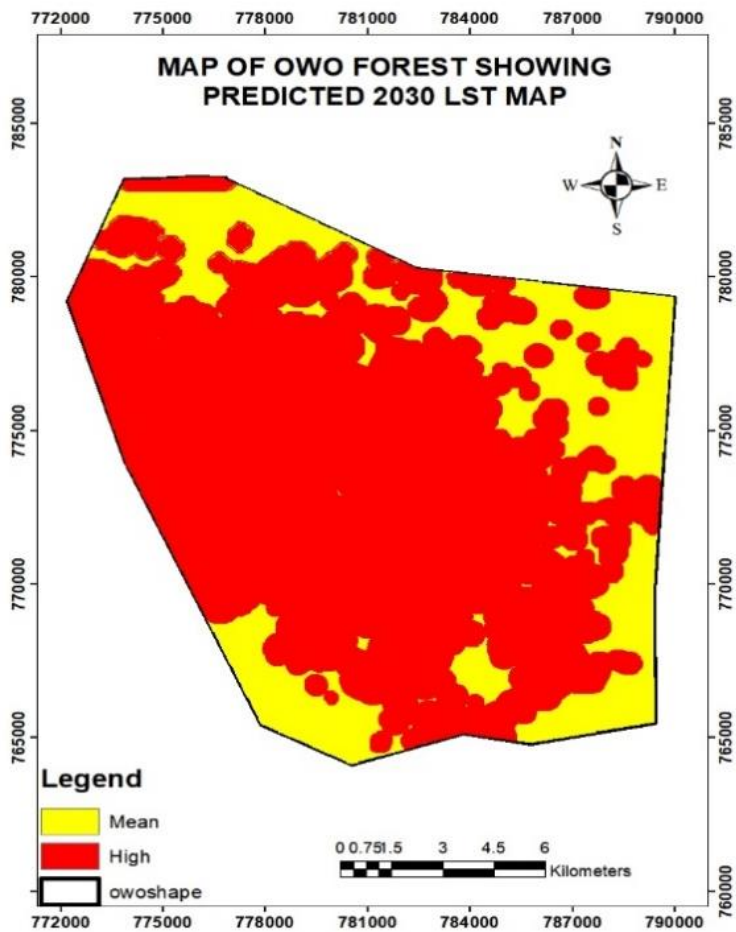


**Figure 8.** Predicted LST map in Owo FRA in the year 2030.

Ondo State should leverage this research as a guide since it is an easier and cost-effective method to map and monitor the vegetation level of Owo FRA, and increase the rate of tree planting and green areas preservation (vegetation) in order to mitigate the soaring rate of LST in the study area.

## CONFLICT OF INTERESTS

The author has not declared any conflict of interests.

## ACKNOWLEDGEMENTS

The author appreciates Mr. Ilesanmi Olowokere and Mrs. Titilade Ruth-Aniyikaye for providing the data and software used in this research. Special thanks to the Geomatic and Remote Sensing research groups for their assistance in proofreading the original manuscript. Lastly, appreciation is extended to the Surveying and Geoinformatics laboratory at the Federal University of Technology, Akure, for providing additional facilities used

in processing the data.

## REFERENCES


Agbor CF, Makinde EO (2018). Land Surface Temperature Mapping Using Geoinformation Techniques. Geoinformatics FCE CTU. doi:10.14311/gi.17.1.2.

Araya YH, Cabral P (2010). Analysis and Modelling of Urban Land Cover Change in Setubal and Sesimbra, Portugal. Remote Sensing 2:1549-1563.

Avdan U, Jovanovska J (2016). Algorithm for Automated Mapping of Land Surface Temperature Using LANDSAT 8 Satellite Data Hindawi Publishing Corporation. Journal of Sensors. doi.org/10.1155/2016/1480307.

Balew A, Korme T (2020). Monitoring land surface temperature in Bahir Dar city and its surrounding using Landsat images. The Egyptian Journal of Remote Sensing and Space Sciences. doi.org/10.1016/j.ejrs.2020.02.001.

Chen L, Sun Y, Saeed S (2018). Monitoring and predicting land use and land cover changes using remote sensing and GIS techniques—A case study of a hilly area, Jiangle, China. PLOS ONE. https://doi.org/10.1371/journal.pone.0200493.

Climate Signals (2023). Global land surface temperature trends and climate change. Available at https://www.climatesignals.org/climate-signals/land-surface-temperature-increase. Visited on 14/6/23

Crago RD, Qualls RJ (2014). Use of land surface temperature to estimate surface energy fluxes: Contributions of Wilfried Brutsaert and collaborators, Water Resources Research 50:3396-3408.

El Garouani M, Amyay M, Lahrach A, Oulidi H (2021). Land Surface Temperature in Response to Land Use/Cover Change Based on Remote Sensing Data and GIS Techniques: Application to Saïss Plain, Morocco. Journal of Ecological Engineering pp. 2299-8993.

European Space Agency (2021). Land Surface Temperature. https://sentinels.copernicus.eu/web/sentinel/user-guides/sentinel-3slstr/overview/geophysical-measurements/land-surface-temperature

Feddema JJ, Oleson KW, Bonan GB, Mearns LO, Buja LE, Meehl GA, Washington WM (2005). The importance of land cover change in simulating future climates. www.sciencemag.org/cgi/content/full/310/5754/1674/DC1

Han H, Yang C, Song J (2015). Scenario Simulation and the Prediction of Land Use and Land Cover Change in Beijing, China. Sustainability-Basel 7(4):4260-4279.

Hashim H, Abd Latif Z, Adnan NA (2019). Urban Vegetation Classification with NDVI Threshold Value Method with Very High Resolution (VHR) Pleiades Imagery. The International Archives of the Photogrammetry, Remote Sensing and Spatial Information Sciences, Volume XLII-4/W16. 6th International Conference on Geomatics and Geospatial Technology (GGT 2019), 1–3 October 2019, Kuala Lumpur, Malaysia. https://doi.org/10.5194/isprs-archives-XLII-4-W16-237-2019.

Hasnat GNT (2021). A Time Series Analysis of Forest Cover and Land Surface Temperature Change Over Dudpukuria-Dhopachari Wildlife Sanctuary Using Landsat Imagery. Frontier Forest Global Change 4:687988.

How Jin Aik D, Ismail MH, Muharam FM, Alias MA (2021). Evaluating the impacts of land use/land cover changes across topography against land surface temperature in Cameron Highlands. PLoS ONE 16(5):e0252111.

Ibrahim I, Abu samah A, Fauzi R, Noor N (2016). The land surface temperature impact to land cover types. ISPRS - International Archives of the Photogrammetry, Remote Sensing and Spatial Information Sciences XLI-B3. 871-876. DOI:10.5194/isprs-archives-XLI-B3-871-2016.

James JM, Abubakar T, Gundiri LR (2020). Impact of Deforestation on Land Surface Temperature in Northern Part of Bauchi State, Nigeria. FUTY Journal of the Environment. Photogrammetry, Remote Sensing and spatial Information Science. Vol. XL-1/W5. http://creativecommons.org/licenses/by/4.0/.

Jeevalakshmi D, Narayana Reddy S, Manikiam B (2017). Land Surface Temperature Retrieval from LANDSAT data using Emissivity Estimation. International Journal of Applied Engineering Research. ISSN 0973-4562.

Lamidi AJ, Ijaware VA (2022). Land Suitability for None-Rice Cultivation Areas in Ekiti State Using a GIS- Based Analytic Hierarchy Process Approach. European Journal of Environment and Earth Science (EJ-GEO) 3(5):51-59. www.sciencepublishinggroup.com/j/ijaas

Meteobox (2021). Owo, Ondo. 5/6/2021. https://meteobox.com/nigeria/owo//

National Aeronautical Space Agency (2008). Land Surface Temperature Product. 6/5/2021. https://modis.gsfc.nasa.gov/gallery/individual.php?db_date=2008-10-27

Mohamadi B, Chen S, Balz T, Gulshad K, McClure SC (2019). Normalized Method for Land Surface Temperature Monitoring on Coastal Reclaimed Areas. MPDI. Sensors. doi:10.3390/s19224836.

Mohd-Jaafar W, Abdul Maulud KN, Kamarulzaman AM, Raihan A, Sah SM, Ahmad A, Saad SN, Mohd Azmi AT, Syukri NK, Khan WR (2020) The Influence of Deforestation on Land Surface Temperature—A Case Study of Perak and Kedah, Malaysia. Forests. MPDI. doi:10.3390/f11060670

Ngie A, Abutaleb K, Ahmed F, Taiwo A, Darwish AA, Ahmed A (2016). An Estimation of Land Surface Temperatures from Landsat ETM+ images for Durban, South Africa. Rwanda Journal. Life and Natural Sciences: Special issue II. doi.org/10.4314/rj.v1i1S.2D.

Odunuga S, Badru G (2015). Landcover Change, Land Surface Temperature, Surface Albedo and Topography in the Plateau Region of North-Central Nigeria. Land 4(2):300-324.

Othman MA, Ash'aari ZH, Ramli M (2018). Tropical deforestation monitoring using NDVI from MODIS satellite: a case study in Pahang**,** *Malaysia.* Environmental Science, Mathematics. IOP Conference Series: Earth and Environmental Science DOI:10.1088/1755-1315/169/1/012047 Corpus ID: 134751947

Shatnawi N, Abu Qdais H (2019). Mapping urban land surface temperature using remote sensing techniques and artificial neural network modelling. International Journal of Remote Sensing. doi: 10.1080/01431161.2018.1557792

Tang B, Zhao X, Zhao W (2018). Local Effects of Forests on Temperatures across Europe. *MPDI.* Remote Sensing. doi:10.3390/rs10040529.

USGS (2014). Landsat Processing Details. Retrieved December 10, 2014, from USGS Landsat Mission Web site: http://landsat.usgs.gov/Landsat_Processing_Details.php

Weather Spark (2021). Average weather in Owo, Nigeria. https://weateher sprk.com/y/51416/Average-weather-in-Owo-Nigeria-Year-Round.

Weng Q (2002). Land Use Change Analysis in the Zhujiang Delta of China using Satellite remote sensing, GIS and stochastic modelling. Journal of Environmental Management 64:273-284. [Crossref] [PubMed] [Web of Science], [Google Scholar].

Weng Q, Lu D, Schubring J (2004). Estimation of land surface temperature–vegetation abundance relationship for urban heat island studies. Elsevier. Remote Sensing of Environment – Elsevier. doi:10.1016/j.rse.2003.11.005.

Zhi Y, Shan L, Ke L, Yang R (2020). Analysis of Land Surface Temperature Driving Factors and Spatial Heterogeneity Research Based on Geographically Weighted Regression Model. Hindawi. Volume 2020, Article ID 2862917. https://doi.org/10.1155/2020/2862917

## Related Journals:




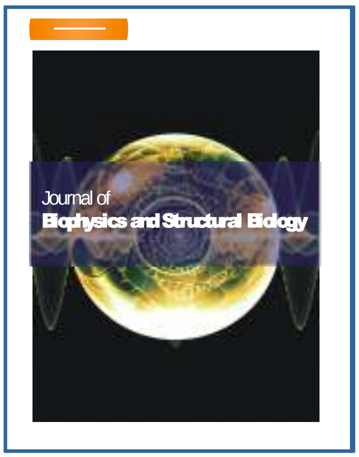







www.academicjournals.org